Inorganic Chemistry

Article

pubs.acs.org/IC

Ligand-Modulated Chemical and Structural Implications in Four-, Five-, and Six-fold Coordinated Aluminum Heteroaryl Alkenolates

Lisa Czympiel,[†] Johannes Pfrommer,[†] Wieland Tyrra,[†] Mathias Schäfer,[‡] and Sanjay Mathur*[,†]

[†]Department of Chemistry, Institute of Inorganic Chemistry and [‡]Department of Chemistry, Institute of Organic Chemistry, University of Cologne, 50939 Cologne, Germany

Supporting Information

ABSTRACT: Synthesis and characterization (gas phase, solution, and solid-state) of a series of four-, five- and six-fold coordinated heteroaryl-alkenolato aluminum complexes were performed to demonstrate the delicate interplay of structural and chemical influences of ligands in the design of new precursors for chemical vapor deposition. We are investigating the properties of heteroaryl alkenols as O^N chelating ligands [where O^N is 3,3,3-trifluoro-(pyridin-2-yl)propen-2-ol (H-PyTFP), 3,3,3-trifluoro(1,3-benzimidazol-2-yl)propen-2-ol (H-BITFP), 3,3,3-trifluoro(dimethyl-1,3-oxazol-2-yl)propen-2-ol (H-DMOTFP), 3,3,3-trifluoro(1,3-benzoxazol-2-yl)propen-2-ol (H-BOTFP), 3,3,3-trifluoro(1,3-benzthiazol-2-yl)propen-2-ol (H-BTTFP), and 3,3,3-trifluoro(dimethyl-1,3-thiazol-2-yl)propen-2-ol (H-DMTTFP)] to prepare volatile and air-stable compounds. All three methyl groups in highly reactive $AlMe_3$ could be replaced by H-PyTFP, H-BITFP, H-DMOTFP, and H-BOTFP yielding octahedral complexes of the type $Al(O^N)_3$; under similar conditions H-BTTFP and H-DMTTFP produced heteroleptic $MeAl(O^N)_2$ compounds with five-fold coordinated aluminum centers. Various attempts to obtain tris-alkenolato derivatives by choosing higher temperatures and prolonged reaction times were not successful. The reaction of H-PyTFP with $[Al(O^tBu)_3]_2$ produced the dimeric heteroleptic $[Al(PyTFP)(O^tBu)_2]_2$ complex with Al atoms present in both octahedral (O_h) and tetrahedral (T_d) coordination in a single molecular unit. The introduction of the chelating ligand H-PyTFP in the dimeric framework of $[Al(O^tBu)_3]_2$ enhanced the stability against hydrolyses significantly. The tendency of Al(III) centers to preferably coordinate in T_d or O_h environment was elucidated by hydrolysis studies of monomeric $Al(PyTFP)_3$, $Al(BOTFP)_3$, and $MeAl(BTTFP)_2$ that produced hydroxo-bridged dimers to retain the octahedral environment for Al atoms. Surprisingly, hydrolysis of monomeric $MeAl(DMTTFP)_2$ yielded an oxo-bridged dimer with two five-fold coordinated aluminum centers. The structural features of all new complexes were investigated in solution, vapor, and solid state by multinuclear NMR spectroscopy, EI-MS spectrometry, and single-crystal X-ray diffraction analyses, respectively.

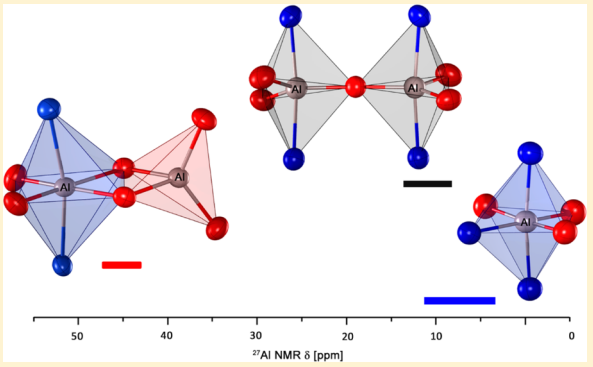

INTRODUCTION

With continuing research interest and increasing technological importance of nanomaterials, particularly thin films of functional materials, the quest for new metal−organic compounds, enabling a controlled synthesis of new materials has gained significant impetus in recent years.[1−5] Aluminum compounds supported by monoanionic alkoxide and β-diketonate ligands are well-known and extensively investigated.[6−18] Among halide and alkyl aluminum complexes, they are the most widely used precursor classes for chemical vapor depositions of Al_2O_3 despite the drawbacks of being prone to hydrolyses or showing low volatilities.[19−26]

In the course of our ongoing efforts toward volatile and air-stable compounds as precursors for metal organic chemical vapor deposition (MOCVD), we are investigating the properties of heteroaryl alkenols as chelating ligands for various metals.[27−29] These aryl-substituted alkenols (N_{Ar}−CH−C-(CF_3)−OH) (Scheme 1**A**) or aryl enaminones (N_{Ar}H−CH−C(CF_3)=O) (Scheme 1**B**) containing different heterocycles exhibit chemical characteristics comparable to those found in β-diketones. However, the possibility of varying the heteroaryl unit in the alkenol backbone allows to create a rational balance of steric and electronic factors that is essential to design new precursors.[1,2,13,30] In addition, the incorporation and variation of $-CF_3$ groups increases the volatility of the compounds by influencing the intermolecular interactions important to control the nuclearity of the molecular compound.

Scheme 1. Schematic Drawing of a Heteroaryl Alkenol A and a Heteroaryl Enaminone B

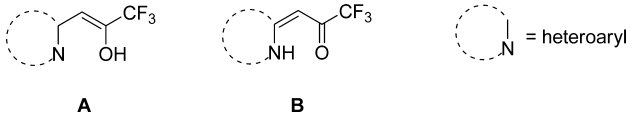

A **B**

Received: March 9, 2014
Published: December 19, 2014

   dx.doi.org/10.1021/ic502549m | *Inorg. Chem.* 2015, 54, 25−37

Copper complexes of 3,3,3-trifluoro(pyridine-2-yl)propen-2-ol were first reported by McGrath and Levine;[31] however, these ligands are only little investigated,[32−37] although an accessible synthesis of various trifluoroacetylazines was reported by Kawase et al.[38] We have improved the synthesis of dimethyloxazol-based ligands and extended the concept to a library of heteroaryl alkenolate ligands based on electronic push−pull effects.[27] The chelating ability of the N_{Ar}−CH−C(R_f)−OH (O^N) backbone and the stability of the resulting six-membered ring offer an interesting option to limit the oligomerization of metal complexes. Our previous efforts showed that metal aryl alkenolates are potential precursors unifying both volatility and air-stability in discrete molecular compounds. For instance the chemical vapor deposition of the tin(II) aryl alkenolate (Sn^{II}(DMOTFP)$_2$) produced high-purity SnO_2 nanowires[27] and did not undergo disproportionation (Sn^{II} → Sn^{IV} + Sn^0) under CVD conditions as reported for [Sn(O^{t}Bu)$_2$]$_2$.[39] The introduction of the trifluoromethyl heteroaryl ligands into dimeric niobium alkoxides produced monomeric derivatives with improved thermal stability and higher volatility making them interesting precursors for deposition of niobium oxide thin films by chemical vapor deposition.[29] Similarly, investigations on palladium(II) and platinum(II) heteroaryl akenolate complexes showed an improved volatility when fluorinated groups (−CF_3 or longer instead of −CH_3) were used possibly due to suppressed intermolecular interactions caused by repulsive forces active between organic peripheries.[28]

Since the presented O^N chelating ligands can possibly coordinate the metal center as monoanionic or neutral ligands, they are of potential interest as redox-active ligand complexes. There has been lots of interest in the field of redox-active main-group-element complexes in recent years,[40−43] especially aluminum complexes containing β-ketoimines,[41,44−46] α-diimines,[43,47−51] and N-heterocyclic carbenes[41] demonstrating unique characteristics and interesting reactivity.

To study the mode of stabilization of the triply charged aluminum ion by aromatic groups and heteroatoms like nitrogen, oxygen, and sulfur, we herein report a series of aluminum chelate complexes with six different heteroaryl alkenolate anions. Through this approach the solid-state and solution structures of new homoleptic and heteroleptic aluminum heteroaryl alkenolate complexes containing four-, five- and six-fold coordinated aluminum centers were obtained.

RESULTS AND DISCUSSION

For the syntheses of the homoleptic Al(O^N)$_3$ as well as the heteroleptic MeAl(O^N)$_2$ and [Al(O^N)(O^{t}Bu)$_2$]$_2$ compounds (O^N = 3,3,3-trifluoro(pyridin-2-yl)propen-2-ol (H-PyTFP), 3,3,3-trifluoro(1,3-benzimidazol-2-yl)propen-2-ol (H-BITFP), 3,3,3-trifluoro(dimethyl-1,3-oxazol-2-yl)propen-2-ol (H-DMOTFP), 3,3,3-trifluoro(1,3-benzoxazol-2-yl)propen-2-ol (H-BOTFP), 3,3,3-trifluoro(1,3-benzthiazol-2-yl)propen-2-ol (H-BTTFP), and 3,3,3-trifluoro(dimethyl-1,3-thiazol-2-yl)-propen-2-ol (H-DMTTFP), see Figure 1) two approaches have been applied (Scheme 2). Homoleptic complexes Al(PyTFP)$_3$, Al(BITFP)$_3$, Al(DMOTFP)$_3$, and Al(BOTFP)$_3$ were prepared analogously to the synthetic approach described by J.-F. Carpentier et al. for the synthesis of Al(hfa)$_3$ (hfa = 1,1,1,5,5,5-hexafluoroacetylacetonate).[52] For this purpose, a stoichiometric amount of the appropriate ligand was added to a solution of $AlMe_3$ in anhydrous toluene. A similar approach has been used for the syntheses of MeAl(DMTTFP)$_2$ and MeAl(BTTFP)$_2$. Through the use of [Al(O^{t}Bu)$_3$]$_2$ as starting material the complexes Al(DMOTFP)$_3$, Al(DMTTFP)$_3$, and the heteroleptic [Al(PyTFP)(O^{t}Bu)$_2$]$_2$ were accessible (Scheme 2).

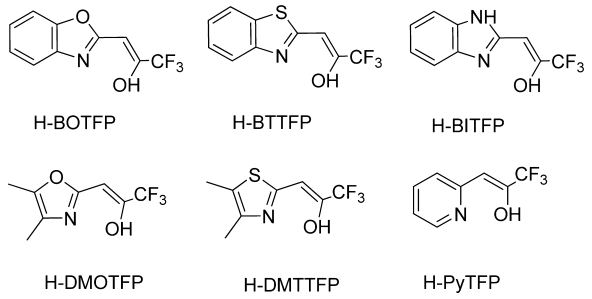

Figure 1. O^N ligands used to prepare Al(O^N)$_3$, MeAl(O^N)$_2$, and [Al(O^N)(O^{t}Bu)$_2$]$_2$ complexes. Abbreviations used throughout the paper are given below the O^N ligands.

All ligands used in this study showed a common ligating mode in which the propenol oxygen and the nitrogen present in the heterocycle coordinated the metal center regardless of the other heteroatom in the ring. Further, the constitution of the heterocycles was found to strongly affect the cleavage of the Al−CH_3 bonds of the starting material $AlMe_3$. For the thiazol ligands H-BTTFP and H-DMTTFP only two Me ligands could be substituted, and the formation of MeAl(BTTFP)$_2$ and MeAl(DMTTFP)$_2$ was observed.

The ^{1}H NMR spectra of the complexes MeAl(DMTTFP)$_2$ and MeAl(BTTFP)$_2$ showed one signal for Al−CH_3 in the range reported for comparable aluminum complexes[53,54] (MeAl(DMTTFP)$_2$: −0.71, MeAl(BTTFP)$_2$: −0.57 ppm). The spectra of both complexes exhibited one set of chelating ligand signals, implying that both the ligands have a similar coordination mode. The ^{1}H,^{1}H-NOESY NMR spectra (Figure 2) showed a cross peak for the protons of the Al−CH_3 to the ligand protons supporting the proposed five-coordinated monomeric alkylaluminum complexes in solution.

Attempts to synthesize Al(BTTFP)$_3$ and Al(DMTTFP)$_3$ starting from $AlMe_3$ by using excess amount of ligands and varying the reaction conditions were not successful, whereas the oxazol derivatives (H-DMOTFP, H-BOTFP) as well as H-BITFP and H-PyTFP selectively formed octahedral Al(O^N)$_3$ complexes with meridional isomers being the predominant product as reported for various asymmetrically substituted tris(β-diketonate)aluminum(III) complexes. The different reaction behavior of the thiazol derivatives toward $AlMe_3$ could be explained by the formation of intermolecular N−H···O hydrogen bonds[55] of neighboring molecules in the ligand structure of H-BTTFP (see Supporting Information) instead of intramolecular hydrogen bonds[56] found in the molecular structure of H-DMOTFP[27] (see Scheme 3). Therefore, a rotation around the C−C single bond adjacent to the heterocycle needs to take place before the ligand can coordinate as a chelate through the enolate oxygen as well as the nitrogen of the heterocycle, and steric hindrance could prevent the coordination of a third ligand (Scheme 3).

All Al(O^N)$_3$ and MeAl(O^N)$_2$ complexes were sparingly soluble in most organic solvents. The products in solid state were stable in ambient atmosphere for several months (NMR evidence); however, they exhibited a high sensitivity toward hydrolysis in solution and formed μ-hydroxide derivatives

dx.doi.org/10.1021/ic502549m | Inorg. Chem. 2015, 54, 25−37

Scheme 2. Schematic Overview of the Synthetic Routes to a Series of $MeAl(O^N)_2$, $Al(O^N)_3$ and $[Al(O^N)(O^tBu)_2]_2$ Complexes

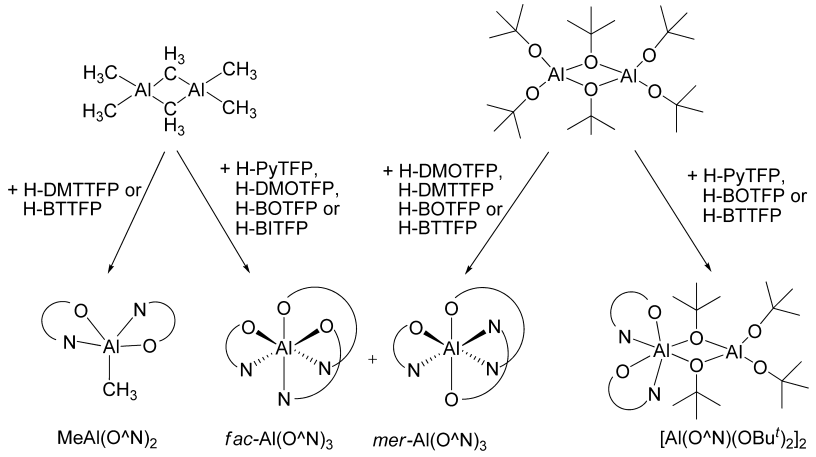

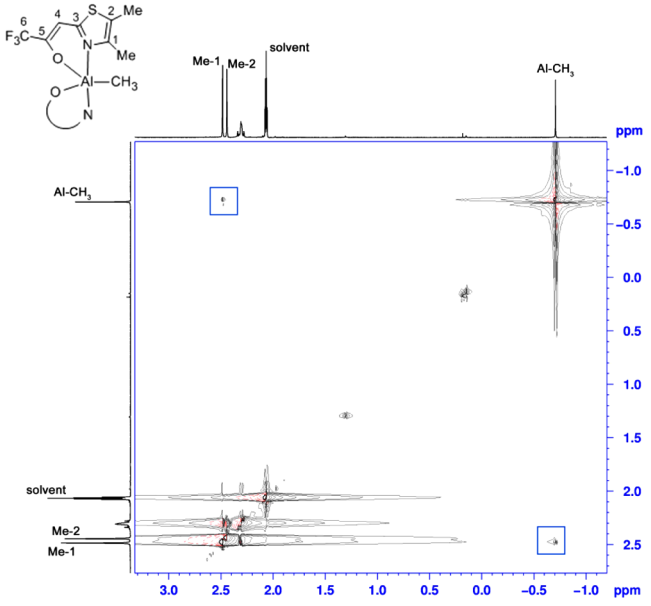

Figure 2. $^1H,^1H$-NOESY spectrum of $MeAl(DMTTFP)_2$ in acetone-d_6 at room temperature.

(Scheme 4) as has already been reported for other O^N and N^N chelating ligands.[42,57−59]

The solution structure of the $Al(O^N)_3$ complexes was established using multinuclear NMR spectroscopy. As reported for various tris(β-diketonate)aluminum(III) complexes[52,60] the *mer* as well as the *fac* isomer of the complexes $Al(O^N)_3$ coexisted in the solution with the *mer* isomer being the predominant product, which could be elucidated by NMR spectroscopy. The facial to meridional ratio of the $Al(O^N)_3$ compounds evaluated by integration of the ^{19}F NMR resonances was ca. 1:99 for $Al(DMOTFP)_3$, 5:95 for $Al(DMTTFP)_3$, 20:80 for $Al(BITFP)_3$, and 25:75 for $Al(BOTFP)_3$ and $Al(PyTFP)_3$. All derivatives displayed analogous spectroscopic characteristics as depicted in Figure 3 by the representative ^1H and ^{19}F NMR spectra of $Al(BOTFP)_3$.

In the minor facial isomer, the three ligands surrounding the aluminum atom are magnetically equivalent due to the inherent C_3 symmetry of the complex. The ^{19}F NMR spectra therefore exhibited a single resonance for this isomer. Additionally, three signals of equal relative intensity and integrative ratio resulted

Scheme 3. (a) Inter- and intramolecular N−H···O hydrogen bonds in H-BTTFP and H-DMOTFP. (b) Proposed reaction mechanism for the formation of $MeAl(BTTFP)_2$

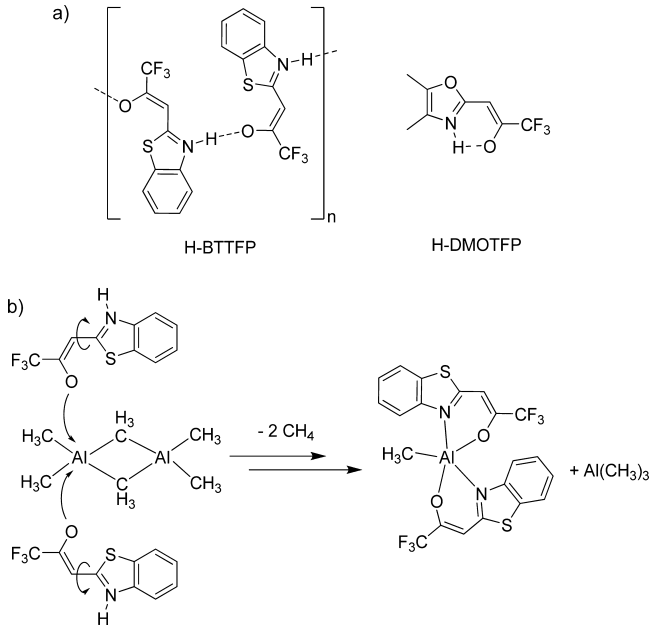

Scheme 4. Hydrolysis of the Octahedral $Al(O^N)_3$ to Form Dimeric $[Al(O^N)_2OH]_2$

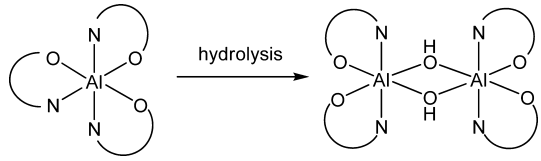

from the predominant meridional isomer of C_1 symmetry, which renders the three O^N ligands chemically and magnetically nonequivalent. Since both isomers are present in solution, the ^1H NMR spectra are expectedly complex due to the overlap of many signals, which were assigned based on a combination of $^{13}C-^{19}F$, $^{13}C-^1H$, and $^1H-^1H$ correlation experiments (see Experimental Section for details). The low solubility of the $Al(BTTFP)_3$ complex as well as the overlap of

dx.doi.org/10.1021/ic502549m | Inorg. Chem. 2015, 54, 25−37

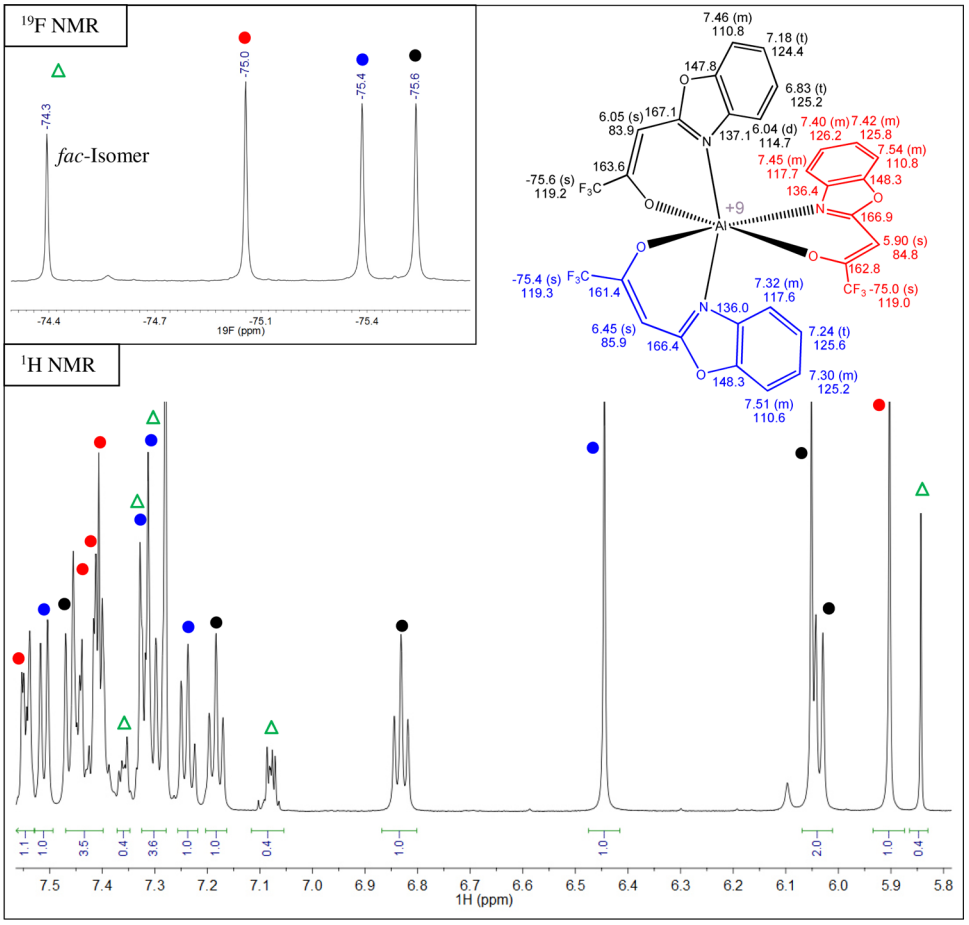

Figure 3. ^{1}H and ^{19}F NMR spectra of $Al(BOTFP)_3$ in $CDCl_3$ at room temperature.

Scheme 5. Proposed Exchange Processes in Solution of $Al(PyTFP)_3$ and $Al(BOTFP)_3$[a]

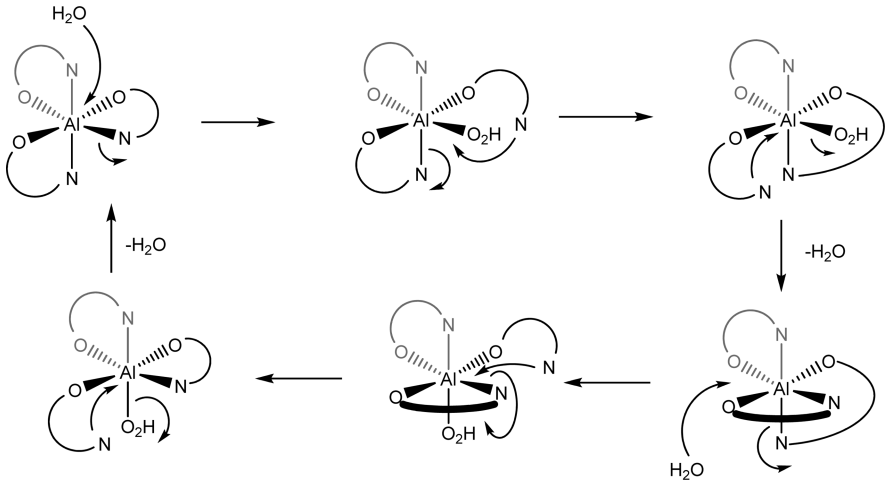

[a]Fixed ligand indicated in grey.

the aromatic signal of the mixture prevented a complete NMR characterization of this compound.

In the ^{1}H and ^{19}F NMR spectra of $Al(PyTFP)_3$ and $Al(BOTFP)_3$ in acetone-d_6 (water content <0.02%) two of the meridional coordinated ligands show broadened peaks implying exchange processes active in solution. The fluxional behavior of the ligands could be explained by the coordination of water to the aluminum center, followed by an Al−N bond cleavage and rearrangement of the ligands, which then causes the elimination of water (Scheme 5).

Similar exchange processes have been found for $Al(acac)_3$ complexes, which were supported by NMR experiments with ^{14}C labeling by Saito and Nagasawa.[61] A proton transfer from water to the unidentate ligand cannot be ruled out as well; however, this mechanism needs further experiments to be reinforced. Apparently, an equilibrium between the $Al(O^N)_3$

dx.doi.org/10.1021/ic502549m | Inorg. Chem. 2015, 54, 25−37

Scheme 6. Synthetic Approach to Heteroleptic $[Al(O^N)(O^tBu)_2]_2$ Complexes

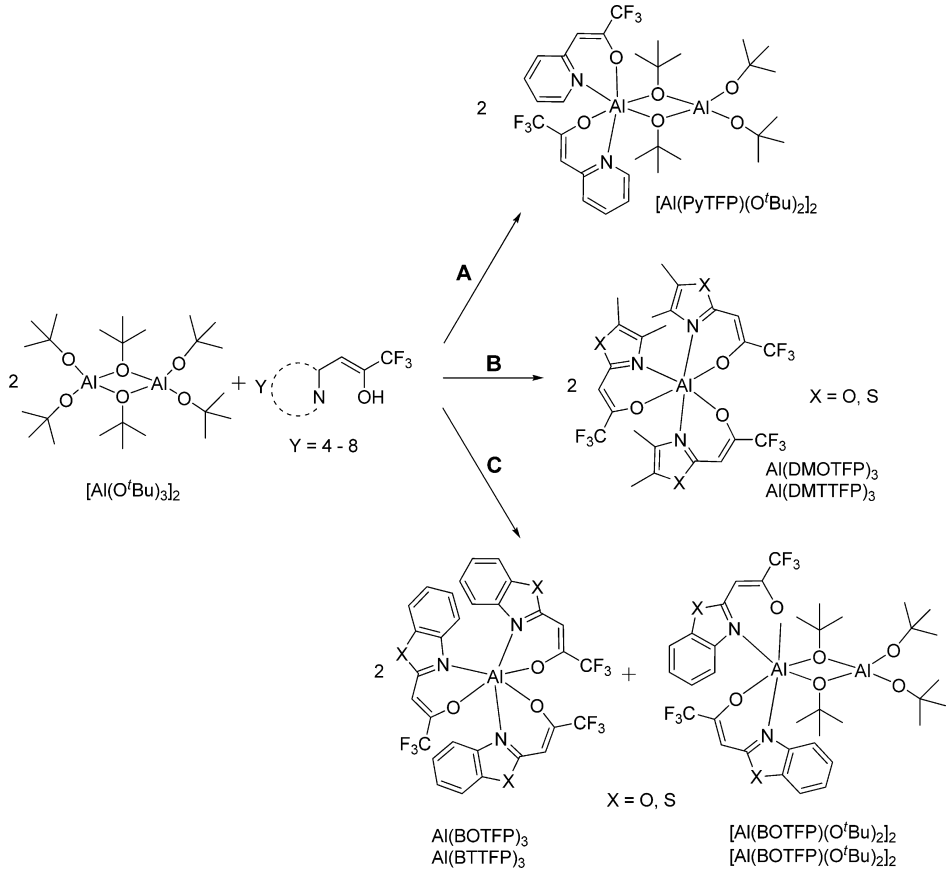

and the hydroxo-bridged compound exists in solution, which slowly shifted toward the more stable hydroxo dimer. The stabilizing effect of small molecules such as acetone or butanone seems to play an important role in this equilibrium since no broadened peaks were detected in NMR spectra (chloroform-d_1) and is further supported by the intercalation of acetone or butanone in the crystal lattice of the hydroxo-bridged complexes $[Al(PyTFP)_2OH]_2$, $[Al(BTTFP)_2OH]_2$, and $[Al(BOTFP)_2OH]_2$ as confirmed by X-ray structure analyses. These hydroxo-bridged dimers were stable under atmospheric conditions and did not undergo further hydrolysis.

All homoleptic $Al(O^N)_3$ complexes exhibited volatility; however, the sublimation temperatures were rather high with $Al(DMOTFP)_3$ displaying the lowest sublimation temperature of 150 °C/10^{-3} mbar. Because of this relatively low volatility the synthesis of heteroleptic alkoxides of aluminum was pursued. Complexes of the type $[Al(O^N)(O^tBu)_2]_2$ were synthesized by ligand exchange reaction using $[Al(O^tBu)_3]_2$ as starting material.

A stoichiometric reaction of $[Al(O^tBu)_3]_2$ and H-PyTFP at ambient temperatures led to the dimeric heteroleptic $[Al(PyTFP)(O^tBu)_2]_2$ (Scheme 6**A**), whereas the reaction with H-DMOTFP and H-DMTTFP at ambient temperature delivered exclusively octahedral $Al(O^N)_3$ complexes (Scheme 6**B**), even if substoichiometric amounts of ligand were used. Reaction of 2 equiv of the ligands H-BOTFP and H-BTTFP with 1 equiv of $[Al(O^tBu)_3]_2$ at ambient temperatures led to a mixture of octahedral $Al(O^N)_3$ and dimeric heteroleptic $[Al(O^N)(O^tBu)_2]_2$ compounds (Scheme 6**C**). It was not possible to influence the reaction in favor of the heteroleptic complexes by reducing the reaction temperature or by changing the ratio of the reactants. Attempts made to separate these species by sublimation or crystallization processes remained unsuccessful.

Compound $[Al(PyTFP)(O^tBu)_2]_2$ with a sublimation temperature of 130 °C/10^{-3} mbar was the only heteroleptic complex that could be isolated in pure form. The good volatility and improved stability in comparison to $[Al(O^tBu)_3]_2$ renders this heteroleptic aluminum alkoxide an interesting precursor for CVD methods. The ^{1}H NMR spectrum of $[Al(PyTFP)(O^tBu)_2]_2$ showed one set of ligand signals for the heteroaryl ligand and two resonances at 1.43 and 1.58 ppm that correspond to the bridging and terminal *tert*-butoxy groups, respectively. The integrative ratio of the ligand signals to the *tert*-butoxy signals of 2:18:18 is consistent with the proposed dimeric structure of the complex.

Interestingly, the reaction of $[Al(O^tBu)_3]_2$ with the thiazol-containing ligands H-BTTFP and H-DMTTFP at ambient temperatures led to the octahedral $Al(DMTTFP)_3$ and $Al(BTTFP)_3$ complexes, which were not accessible from the reaction starting with $AlMe_3$. The formation of the homoleptic octahedral $Al(O^N)_3$ complexes resulting from $[Al(O^tBu)_3]_2$ can be explained by the intermediary formation of $[Al(O^N)(O^tBu)_2]_2$ with a $\{Al(O^tBu)_4\}^-$ moiety,[62,63] which is subsequently substituted by a third monoanionic chelating O^N ligand. Depending on steric effects of the O^N ligand either homoleptic $Al(O^N)_3$ or heteroleptic $[Al(O^N)(O^tBu)_2]_2$ is preferably formed.

The chemical shift in the ^{27}Al NMR spectra is an indicator for the coordination number of the aluminum atom (Figure 4). Hexacoordinated aluminum compounds are found at highest field with the smallest half-line widths, whereas four- and five-coordinated aluminum compounds are shifted significantly

dx.doi.org/10.1021/ic502549m | *Inorg. Chem.* 2015, 54, 25−37

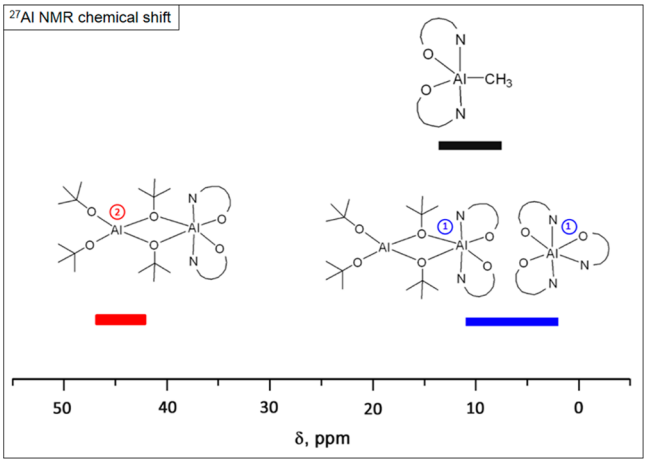

Figure 4. Correlation of coordination numbers of the metal atoms in the Al complexes with their chemical shifts in ^{27}Al NMR spectra.

downfield as broad diffuse signals with half-line widths often exceeding 10^3 Hz.[64−68] The complexes Al(O^N)$_3$ showed resonances in the range of 6−9 ppm in acetone-d_6 indicating octahedral ligand arrangement confirming that the 3-fold arrangement of bidentate ligand observed in the solid state is retained in solution.[67] The signals of the pentacoordinated complexes MeAl(O^N)$_2$ were particularly difficult to detect due to the low solubilities of the derivatives and broad diffuse signals. By subtracting the baseline of an Al-free sample from that of an Al-containing sample it was possible to determine the shifts of 13 ppm (MeAl(DMTTFP)$_2$) and 10 ppm (MeAl(BTTFP)$_2$) with a half-line width of 4000 and 5000 Hz, respectively. For the complex [Al(PyTFP)(O^{t}Bu)$_2$]$_2$, the ^{27}Al NMR spectrum showed two signals attributable to octahedrally (8 ppm) and tetrahedrally coordinated aluminum (45 ppm), which correspond well with the chemical shifts found for the related binuclear aluminum complex [(C$_6$H$_4$O{CH═N-(C$_6$H$_5$)})Al(O^{i}Pr)$_2$]$_2$.[69]

Electron Impact Mass Spectrometry. In the homoleptic derivatives Al(O^N)$_3$ as well as in the MeAl(O^N)$_2$ complexes, the radical cations [Al(O^N)$_2$]$^+$ exhibited ions of highest abundance in the electron impact mass spectrometry (EI-MS) (20 eV) spectra. The molecular ion peaks (M$^+$) of Al(O^N)$_3$ were detected with an intensity ranging from 4% (Al(BITFP)$_3$) to 20% (Al(BOTFP)$_3$) suggesting a superior stability of the tetrahedral coordinated complex ions [Al(O^N)$_2$]$^+$ in the gas phase, which has been extensively studied by IRMPD spectroscopy and computational modeling.[70] The cationic [Al(O^N)$_2$]$^+$ species adopt tetrahedral arrangements with two bidentate ligands arranged around the central main group metal cation coordinating through the negatively charged enolate oxygen and the Lewis-basic nitrogens of the heterocycles.[70]

The EI-MS spectra of [Al(BOTFP)$_2$(OH)$_2$]$_2$ also showed tetrahedrally coordinated radical ion [Al(O^N)$_2$]$^+$ with highest intensity. Furthermore, two peaks for dimeric structures can be found at m/z = 982 with significant intensities of 28% and m/z = 754 of 36%. These ions correspond to the oxo-bridged complexions [Al$_2$(BOTFP)$_4$O]$^+$ and [Al$_2$(BOTFP)$_3$O]$^+$, respectively.

In the mass spectra of the heteroleptic dimeric compound [Al(PyTFP)(O^{t}Bu)$_2$]$_2$ no evidence is found for the M$^+$ peak. The fragment with highest mass at m/z = 707 and intensity of 12% corresponds to the ion [M −CH$_3$]$^+$. The signals at m/z = 593 (20%) and m/z = 577 (16%) are best explained through loss of two −C(CH$_3$)$_3$ and an additional −CH$_3$ group. The most intensive peak corresponded to [Al$_2$(PyTFP)(O^{t}Bu)$_4$]$^+$ (m/z = 534); further loss of one CH$_3$ fragment led to the peak at m/z = 519 with an intensity of 34%. All other peaks at m/z = 478, 422, 366, and 310 corresponded to further loss of −CH$_3$ and −C(CH$_3$)$_3$ fragments. Moreover, the tetrahedrally coordinated complex ion [Al(O^N)$_2$]$^+$ was detected at m/z = 403 with an intensity of 8%.

Solid-State Structures. The different hydrolysis behavior of the Al(O^N)$_3$ complexes was also apparent during the crystallization process. It was possible to obtain single crystals suitable for X-ray diffraction analyses for Al(DMOTFP)$_3$ from acetone at 4 °C, whereas all other compounds formed microcrystalline materials unsuitable for X-ray diffraction analyses. After addition of small amounts of water single crystals of [Al(BOTFP)$_2$OH]$_2$·2(C$_4$H$_8$O) from butanone solution, and [Al(PyTFP)$_2$OH]$_2$·2(C$_3$H$_6$O), [Al(BTTFP)$_2$OH]$_2$·2(C$_3$H$_6$O), and [Al(DMTTFP)]$_2$O from acetone were obtained upon storing for several days at 4 °C. The ^{1}H NMR spectrum of crystals of [Al(BOTFP)$_2$OH]$_2$ grown from butanone showed one set of signals for the coordinated ligands, a broad peak at 3.68 ppm, which corresponds to the bridging hydroxy groups, as well as signals for butanone. The pattern of this NMR spectrum, which differs substantially from NMR spectra of the freshly dissolved Al(O^N)$_3$ compounds, endorses the initial existence of the homoleptic Al(O^N)$_3$ complexes in solution and their slow hydrolysis to [Al(O^N)$_2$OH]$_2$. Crystals of [Al(PyTFP)(O^{t}Bu)$_2$]$_2$ were grown from *n*-heptane at −20 °C.

The solid-state structures of [Al(PyTFP)$_2$OH]$_2$·2(C$_3$H$_6$O), [Al(BOTFP)$_2$OH]$_2$·2(C$_4$H$_8$O), and [Al(BTTFP)$_2$OH]$_2$·2(C$_3$H$_6$O) (Figure 5) displayed a central dimeric unit formed by μ-bridging hydroxy groups with aluminum centers resembling distorted octahedral. In all the molecular structures, the N atoms of the ligands reside in axial positions. From the possible isomers for a symmetric dimer (*meso* and *d,d/l,l* forms, Scheme 7) only the chiral isomer was found. Selected crystallographic data and collection parameters for these compounds are presented in Table 1.

The octahedral environment is substantially distorted from ideal parameters in all three compounds, with *cis* and *trans* angles varying from 74.1(3)° to 98.64(10)° and 167.40(20)° to 168.86(8)°. The Al−O bond lengths involving the chelating ligands are longer in [Al(BOTFP)$_2$OH]$_2$·2(C$_4$H$_8$O) (1.861(1) Å and 1.866(2) Å) than in [Al(PyTFP)$_2$OH]$_2$·2(C$_3$H$_6$O) and [Al(BTTFP)$_2$OH]$_2$·2(C$_3$H$_6$O) (1.841(3) Å to 1.844(5) Å). On the contrary, the Al−O distances concerning the μ-bridging hydroxides were slightly longer in [Al(PyTFP)$_2$OH]$_2$·2(C$_3$H$_6$O) (1.875(3) Å, 1.873(3) Å) than in [Al(BOTFP)$_2$OH]$_2$·2(C$_4$H$_8$O) (1.864(2) Å, 1.857(2) Å) and [Al(BTTFP)$_2$OH]$_2$·2(C$_3$H$_6$O) (1.866(5) Å, 1.870(5) Å) and differed from related complexes such as [Al(hfa)$_2$(OH)]$_2$ (1.831(2) Å).[52] The Al−N bond lengths lie in the range of 2.042(2) to 2.057(2) Å for [Al(BOTFP)$_2$OH]$_2$·2(C$_4$H$_8$O), 2.071(3) to 2.091(3) Å for [Al(PyTFP)$_2$OH]$_2$·2(C$_3$H$_6$O) and 2.123(5) to 2.128(5) Å for [Al(BTTFP)$_2$OH]$_2$·2(C$_3$H$_6$O).

The hydrolysis of the MeAl(DMTTFP)$_2$ compound led to an oxo-bridged centrosymmetric derivative [Al(DMTTFP)$_2$]O with two aluminum centers coordinated by two DMTTFP ligands each and an oxo-bridge connecting the two aluminum centers (Figure 6, Table 2). The Al-(μ-O) bond distance of 1.688(2) Å is in accordance with literature known [Al(O^N)$_2$]$_2$O complexes.[71−73] In order to examine the distortion

dx.doi.org/10.1021/ic502549m | *Inorg. Chem.* 2015, 54, 25−37

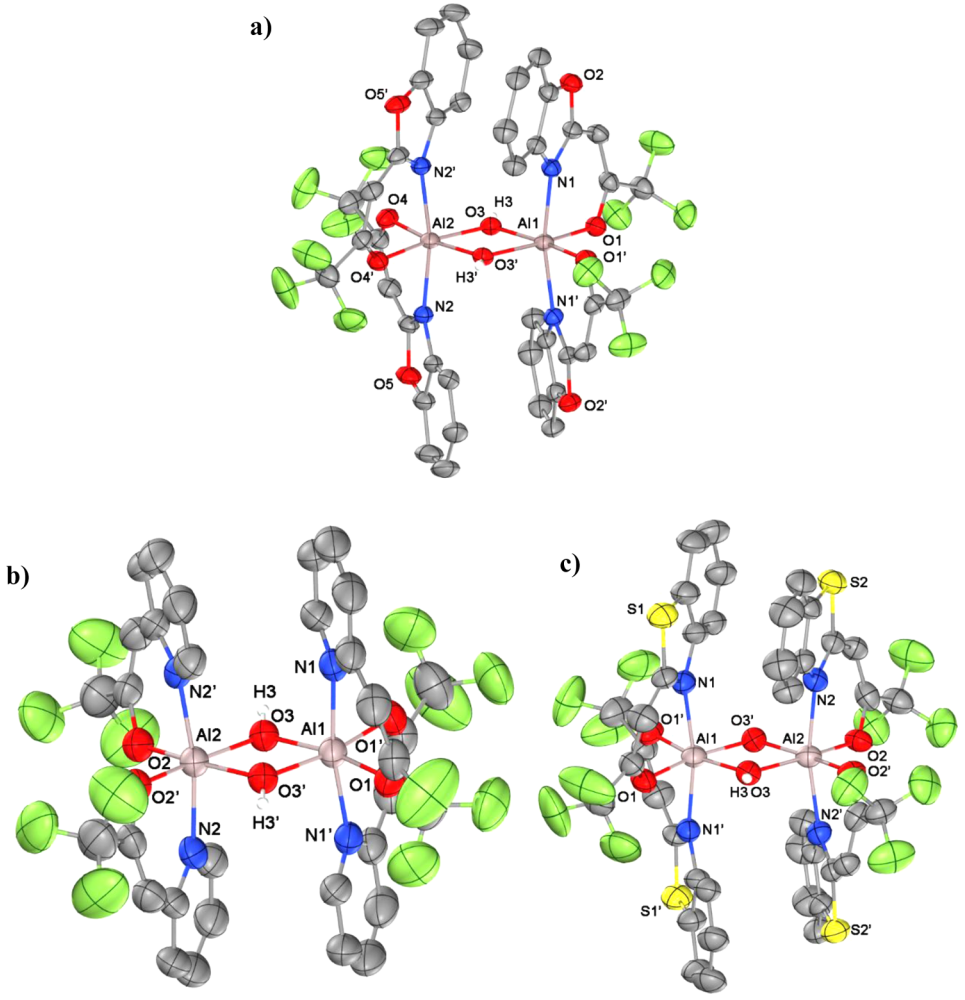

Figure 5. Molecular structures of $[Al(BOTFP)_2OH]_2 \cdot 2(C_4H_8O)$ (a), $[Al(PyTFP)_2OH]_2 \cdot 2(C_3H_6O)$ (b) and $[Al(BTTFP)_2OH]_2 \cdot 2(C_3H_6O)$ (c) with the corresponding atom labeling scheme. Thermal ellipsoids are drawn at the 50% probability level; the lattice acetone and butanone as well as all hydrogen atoms, except OH groups, have been omitted for clarity. Selected bond lengths (Å) and angles (deg): (a) Al1−O1 1.8609(15), Al1−O3 1.8640(16), Al1−N1 2.0416(16), Al2−O3 1.8576(16), Al2−O4 1.8670(16), Al2−N2 2.0562(17), Al1−Al2 2.9411(12); O1−Al1−O1′ 98.64(10), O1−Al1−O3 92.99(7), O1−Al1−O3′ 168.27(8), O3′−Al1−O3 75.43(10), O1−Al1−N1 87.46(7), O1′−Al1−N1 84.50(7), O3−Al1−N1 94.56(7), O3′−Al1−N1 95.19(7), N1−Al1−N1′ 167.66(10), O3′−Al2−O3 75.74(10), O3′−Al2−O4 168.86(8), O3−Al2−O4 93.32(7), O3−Al2−N2′ 95.02(7), O3′−Al2−N2′ 93.95(7), O4−Al2−O4′ 97.68(11), O4−Al2−N2′ 84.80(7), O4′−Al2−N2′ 87.73(7), N2′−Al2−N2 168.64(10), Al2−O3−Al1 104.42(8). (b) Al1−O1 1.844(3), Al1−O3 1.875(3), Al1−N1 2.071(3), Al2−O2 1.841(3), Al2−O3 1.873(3), Al2−N2 2.091(3), Al1−Al2 2.971(2); O1−Al1−O1′ 95.9(2), O1′−Al1−O3 94.64(14), O1−Al1−O3 169.00(15), O3−Al1−O3′ 75.06(19), O1′−Al1−N1′ 88.82(14), O1−Al1−N1′ 84.65(14), O3−Al1−N1′ 92.37(13), O3′−Al1−N1′ 95.36(14), N1′−Al1−N1 170.3(2), O2′−Al2−O2 96.5(2), O2′−Al2−O3 168.86(15), O2−Al2−O3 94.26(14), O3−Al2−O3′ 75.18(19), O2′−Al2−N2 88.87(14), O2−Al2−N2 84.36(14), O3−Al2−N2 95.11(14), N2−Al2−N2′ 169.8(2), Al2−O3−Al1 104.88(16). (c) Al1−O1 1.844(5), Al1−O3 1.866(5), Al1−N1 2.123(5), Al2−O2 1.843(5), Al2−O3 1.870(5), Al2−N2 2.128(5); O1−Al1−O1′ 96.8(3), O1−Al1−O3 94.6(2), O1−Al1−O3′ 168.4(2), O3−Al1−O3′ 74.3(3), O1−Al1−N1 87.8(2), O1−Al1−N1′ 84.7(2), O3−Al1−N1 93.10(19), O3−Al1−N1′ 95.9(2), N1−Al1−N1 168.8(3), O2−Al2−O2′ 98.1 (3), O2−Al2−O3 167.4(2), O3−Al2−O3′ 74.1(3), O2−Al2−N2 88.1(2), O2−Al2−N2′ 83.9(2), O3−Al2−N2 96.4(2), O3−Al2−N2′ 93.3(2), N2−Al2−N2′ 167.8(3), Al1−O3−Al2 105.8(2).

Scheme 7. Possible Isomers for $[Al(O^N)_2OH]_2$

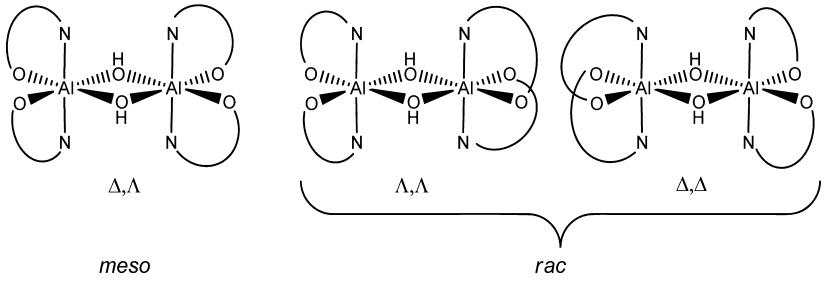

dx.doi.org/10.1021/ic502549m | Inorg. Chem. 2015, 54, 25−37

Table 1. Selected Crystallographic Data and Collection Parameters for Compounds $[Al(BOTFP)_2OH]_2{\cdot}2(C_4H_8O)$, $[Al(PyTFP)_2OH]_2{\cdot}2(C_3H_6O)$, and $[Al(BTTFP)_2OH]_2{\cdot}2(C_3H_6O)$

compound	$[Al(BOTFP)_2OH]_2{\cdot}2(C_4H_8O)$	$[Al(PyTFP)_2OH]_2{\cdot}2(C_3H_6O)$	$[Al(BTTFP)_2OH]_2{\cdot}2(C_3H_6O)$
cryst. syst.	orthorhombic	monoclinic	orthorhombic
space group	*Pbcn*	*C*2/*c*	*Pbcn*
cell parameter	*a* = 15.9790 (5) Å	*a* = 22.9628 (17) Å	*a* = 15.3683 (18) Å
	b = 13.8817 (6) Å	*b* = 14.2750 (7) Å	*b* = 14.4592 (18) Å
	c = 22.4336 (8) Å	*c* = 14.1070 (9) Å	*c* = 23.252 (2) Å
		β = 107.697 (5)°	
Z	4	4	4
total reflns	57 150	29 330	48 594
unique reflns	5088	4339	4376
*R*1, w*R*2 [$I_0 > 2\sigma(I)$]	0.0551, 0.1577	0.0935, 0.1861	0.0710, 0.1347
*R*1, w*R*2 [all data]	0.0590, 0.1618	0.1472, 0.2010	0.1842, 0.1697
GOF	1.047	1.626	0.922
CCDC	956241	956242	956243

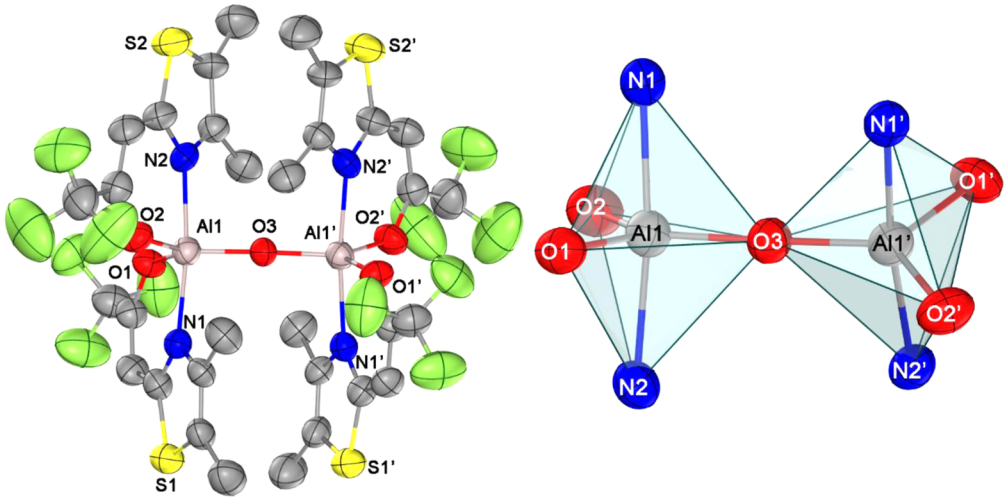

Figure 6. Molecular structure of $[Al(DMTTFP)_2]O$ with atom labeling scheme. Thermal ellipsoids are drawn at the 50% probability level. Protons have been omitted for clarity. Selected bond lengths (Å) and angles (deg): Al1−O1 1.796(4), Al1−O2 1.797(3), Al1−O3 1.688(2), Al1−N1 2.086(4), Al1−N2 2.104(4); O1−Al1−O2 114.69(17), O1−Al1−O3 121.31(14), O2−Al1−O3 124.00(16), O1−Al1−N1 90.03(17), O2−Al1−N1 86.90(15), O3−Al1−N1 93.76(19), O1−Al1−N2 87.33(16), O2−Al1−N2 88.72(16), O3−Al1−N2 92.75(19), N1−Al1−N2 173.45(17).

Table 2. Selected Crystallographic Data and Collection Parameters for Compounds $[\{Al(DMTTFP)_2\}_2O]$, $[Al(PyTFP)(O^tBu)_2]_2$, and $Al(DMOTFP)_3$

compound	$[Al(DMTTFP)_2]_2O$	$[Al(PyTFP)(O^tBu)_2]_2$	$Al(DMOTFP)_3$
cryst. syst.	monoclinic	monoclinic	orthorhombic
space group	*C*2/*c*	$P2_1/c$	*Pbca*
cell parameter	*a* = 10.6761 (18) Å	*a* = 10.7308 (11) Å	*a* = 16.9876 (4) Å
	b = 26.194 (6) Å	*b* = 20.052 (3) Å	*b* = 17.7901 (6) Å
	c = 15.456 (3) Å	*c* = 20.203 (2) Å	*c* = 18.8103 (5) Å
	β = 108.469 (13)°	*β* = 121.644 (7)°	
Z	4	4	8
total reflns	20 735	40 627	65 666
unique reflns	5514	8257	6048
*R*1, w*R*2 [$I_0 > 2\sigma(I)$]	0.0493, 0.0635	0.0674, 0.1749	0.0557, 0.1634
*R*1, w*R*2 [all data]	0.2439, 0.0937	0.1203, 0.1974	0.0734, 0.1816
GOF	0.675	0.926	1.049
CCDC	956244	956245	956240

of the coordination geometry, the value τ, which measures how closely a distorted five-coordinate compound approximates either a trigonal bipyramidal or square pyramidal geometry, was calculated according to the reported method.[74] The value of τ = 0.82 suggested that the geometry around the aluminum centers is best described as distorted trigonal bipyramidal. The Al−O (1.796(4) and 1.797(3) Å) and Al−N (2.086(4) and 2.104(4) Å) bond distances are similar to the average distances observed for other structurally characterized aluminum complexes containing O^N ligands.[53,71−73,75]

The molecular structure of $Al(DMOTFP)_3$ (Figure 7, Table 2) exhibited the central aluminum atom in an octahedral environment. In accordance with the NMR data only the *mer* isomer of this complex was found in the solid-state. The octahedral spatial arrangement around aluminum is slightly distorted with *cis* and *trans* angles ranging from 85.65° to 95.35° and 173.9° to 175.3°, respectively. The Al−O bond distance of 1.85−1.87 Å as well as the Al−N bond lengths of 2.02−2.05 Å are in the range of bond lengths found in related aluminum derivatives.[76,77]

The dimeric structure of $[Al(PyTFP)(O^tBu)_2]_2$ is built by one octahedrally coordinated aluminum center substituted by two O^N ligands and one tetrahedrally coordinated aluminum

dx.doi.org/10.1021/ic502549m | *Inorg. Chem.* 2015, 54, 25−37

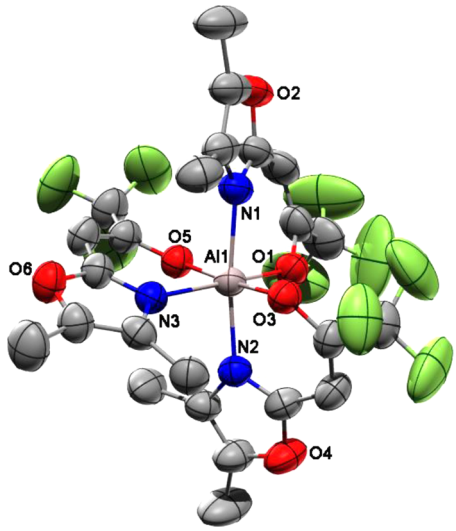

Figure 7. Molecular structure of $Al(DMOTFP)_3$ with atom labeling scheme. Thermal ellipsoids are drawn at the 50% probability level; all hydrogen atoms have been omitted for clarity. Selected bond lengths (Å) and angles (deg): Al1−O1 1.851(2), Al1−O3 1.837(2), Al1−O5 1.855(2), Al1−N1 2.052(2), Al1−N2 2.026(2), Al1−N3 2.050(2); O3−Al1−O1 93.89(8), O3−Al1−O5 175.30(9), O5−Al1−O1 87.53(8), O1−Al1−N1 88.57(8), O3−Al1−N1 86.45(9), O5−Al1−N1 89.11(9), O1−Al1−N2 86.19(8), O3−Al1−N2 89.75(8), O5−Al1−N2 94.82(8), O1−Al1−N3 173.76(9), O3−Al1−N3 91.95(8), O5−Al1−N3 86.80(8), N2−Al1−N1 173.30(9), N2−Al1−N3 91.68(8), N3−Al1−N1 93.96(8).

atom with two terminal *tert*-butoxy groups and two μ-bridging *tert*-butoxy groups (Figure 8, Table 2). This structure motive has been observed in $[Al(OR)_2(\beta\text{-diketonate})]_2$ complexes like $[Al(O^iPr)_2(acac)]_2$[78,79] or $[Al(O^iPr)_2(^tbuac)]_2$[80] with gradual bong length variation among: (a) the terminal *tert*-butoxy groups with bond-lengths of 1.683(2) and 1.679(3) Å, (b) the bridging *tert*-butoxy groups bound to the tetrahedrally coordinated aluminum center with a bond length of 1.819(2) and 1.820(2) Å and (c) the bridging *tert*-butoxy groups bound to the octahedrally coordinated aluminum center with a bond length of 1.916(2) and 1.914(2) Å. The longer bond lengths of the bridging butoxy groups to the 6-fold coordinated aluminum atom could be explained by the steric demand of the PyTFP ligands. The Al−N (2.10 and 2.08 Å) as well as the Al−O (1.84 Å) bond lengths involving the chelating ligands were similar to those found in $[Al(PyTFP)_2OH]_2\cdot 2(C_3H_6O)$. The edge-linkage between the two polyhedra together with the steric demand of all ligands causes severe distortions of the octahedron as well as the tetrahedron evident in the acute angles of 76.35(10)° (O1−Al2−O2) deviating by approximately 14° from an ideal octahedron (90°) and even more by around 28° (81.05°; O1−Al1−O2) from values for a regular tetrahedron (109.47°).

Chemical Vapor Deposition. First CVD experiments with $[Al(PyTFP)(O^tBu)_2]_2$ as precursor resulted in the formation of Al_2O_3 films on Si substrates (Figure 9). With a substrate temperature of 700 °C and a precursor temperature of 150 °C in an ultrahigh vacuum CVD reactor (10^{-6} mbar) a film thickness of 202 ± 5 nm was achieved after a process time of 30 min. The enhanced air stability of the complex in comparison to $[Al(O^tBu)_3]_2$ and $AlMe_3$ greatly facilitated the homogeneity of the coatings obtained from the CVD process. Further investigations regarding the utilization of this heteroleptic complex in deposition of barrier coatings are currently underway.

CONCLUSION

New aluminum complexes based on heteroaryl alkenol ligands (O^N) with 4-, 5- and 6-fold coordinated Al centers were obtained and structurally characterized. The complete elucidation of the solid-state and solution structures together with earlier published investigations of the gas-phase behavior under mass spectrometric conditions allowed a deep insight into the characteristics of this class of compounds. Through different reaction routes starting from either $AlMe_3$ or $[Al(O^tBu)_3]_2$ a selection of $Al(O^N)_3$, $MeAl(O^N)_2$, $[Al(O^N)(O^tBu)_2]_2$, and $[Al(O^N)_2OH]_2$ was accessible. The

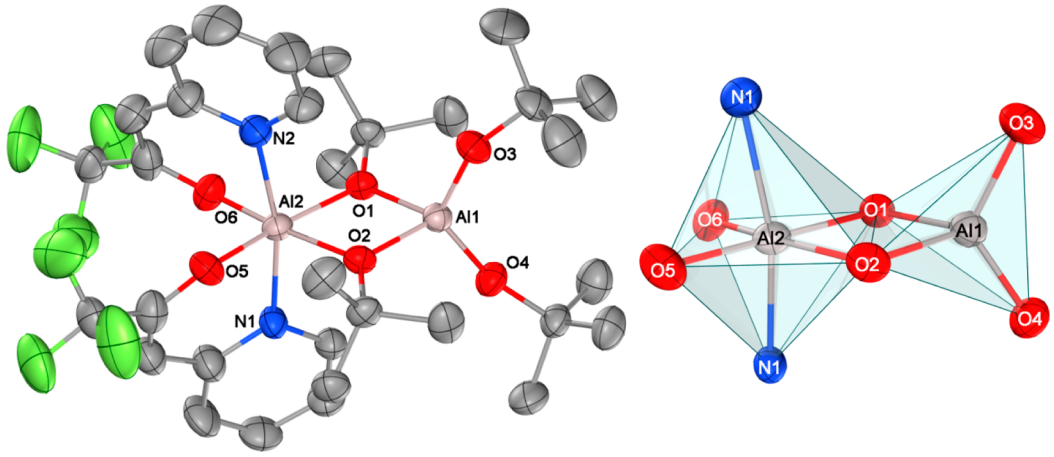

Figure 8. Molecular structure of $[Al(PyTFP)(O^tBu)_2]_2$ with atom labeling scheme. Thermal ellipsoids are drawn at the 50% probability level. Protons have been omitted for clarity. Selected bond lengths (Å) and angles (deg): Al2−O6 1.836(3), Al2−O5 1.842(3), Al2−O2 1.916(2), Al2−O1 1.914(2), Al2−N2 2.081(3), Al2−N1 2.102(3), Al1−O2 1.819(2), Al1−O1 1.820(2), Al1−O3 1.679(3), Al1−O4 1.683(2); O6−Al2−O5 94.57(12), O6−Al2−O2 170.46(12), O6−Al2−O1 94.65(11), O5−Al2−O2 94.65(11), O5−Al2−O1 170.47(12), O2−Al2−O1 76.25(10), O6−Al2−N2 88.81(12), O5−Al2−N2 83.17(12), O2−Al2−N2 94.70(11), O1−Al2−N2 94.59(11), O6−Al2−N1 83.04(12), O5−Al2−N1 88.20(13), O2−Al2−N1 94.83(11), O1−Al2−N1 95.33(12), N2−Al2−N1 167.62(12), Al2−O2−Al1 101.30(11), O2−Al1−O1 81.05(11), O2−Al1−O3 110.90(12), O2−Al1−O4 111.62(13), O1−Al1−O3 113.86(13), O1−Al1−O4 110.38(12), O3−Al1−O4 121.81(13).

dx.doi.org/10.1021/ic502549m | Inorg. Chem. 2015, 54, 25−37

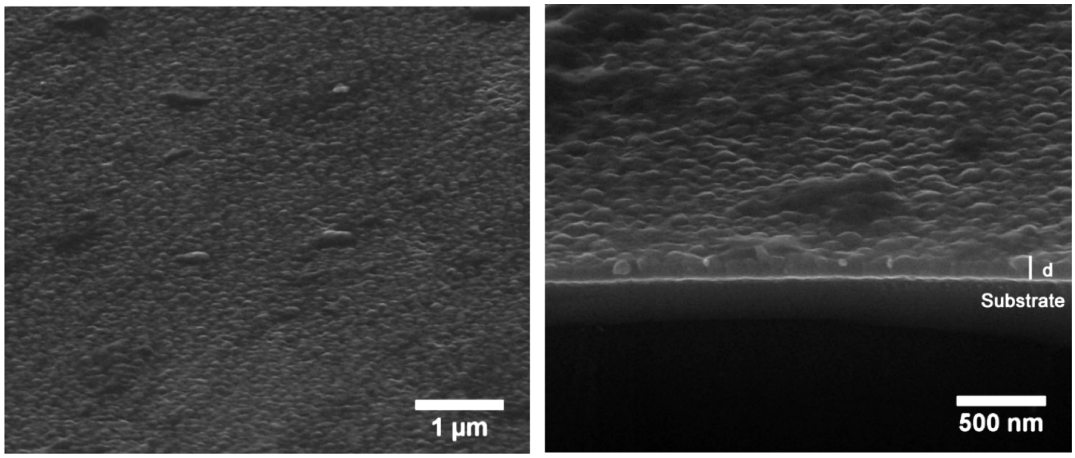

Figure 9. (a) SEM image of as-deposited Al_2O_3 film on a Si substrate. (b) Cross-section image of as-deposited Al_2O_3 film on a Si substrate (d = 202 ± 5 nm).

tris-heteroaryl alkenolate derivatives, $Al(O^{\wedge}N)_3$, showed higher stability as solids in air but tend to hydrolyze in solution to yield the hydroxo-bridged dimers $[Al(O^{\wedge}N)_2OH]_2$ resistant toward further hydrolysis.

The results presented here demonstrate the delicate interplay of steric factors and intermolecular interactions during the formation of these aluminum compounds. Especially the inter- and intramolecular hydrogen bonds in the molecular structures of the O^N ligands influenced the molecular composition of the formed homo- and heteroleptic aluminum complexes as could be shown for the reaction of H-BTTFP with $AlMe_3$. Homoleptic $Al(O^{\wedge}N)_3$ and methyl-substituted $MeAl(O^{\wedge}N)_2$ compounds exhibited limited volatility, whereas partial substitution of alkoxy ligands in $[Al(O^tBu)_3]_2$ yielded the heteroleptic dimeric compound $[Al(PyTFP)(O^tBu)_2]_2$, which is convenient to handle in contrast to simple alkoxides. This complex displays promising properties like good volatility and adequate stability in the gas phase as well as easy accessibility in high yields and purity. First CVD experiments resulted in the deposition of Al_2O_3 at moderate conditions (Figure 9), which supports our molecule-based approach to nanostructured materials.

EXPERIMENTAL SECTION

All manipulations of air- and moisture-sensitive materials were carried out under nitrogen using Stock-type all glass assemblies. The ligands H-PyTFP, H-BITFP, H-DMOTFP, H-BOTFP, H-BTTFP (see Supporting Information), and H-DMTTFP were prepared by modifying the procedure described by Kawase et al.[38] As previously reported the purification process was improved by sublimation of the products instead of column chromatography.[27] Solvents were dried by standard methods with appropriate desiccating reagents and distilled prior to their use. Acetone (extra dry, water < 50 ppm) and $AlMe_3$ (1.0 M solution in heptane), were procured from Acros Organics and used without further purification. Elemental analyses were performed on a HEKAtech CHNS Euro EA 3000. Mass spectra were obtained on a Finnigan MAT 95 (20 eV) in *m/z* (rel.%). NMR spectra were recorded either on a Bruker Avance II 300, Bruker AV 400 or on a Bruker Avance II$^+$ 600 spectrometer; chemical shifts are quoted in part per million relative to external TMS (^1H and ^{13}C), $Al(H_2O)_6^{3+}$ (^{27}Al), and CCl_3F (^{19}F). The numbering for the ligands used throughout the experimental section is displayed in Scheme 8.

Data collection for X-ray structure elucidation was performed on STOE IPDS I/II diffractometer using graphite-monochromated Mo Kα radiation (0.710 73 Å). The data were corrected for Lorentz and polarization effects. A numerical absorption correction based on crystal-shape optimization was applied for all data. The programs used in this work are STOE's X-Area, including X-RED[81] and X-Shape[82] for data reduction and absorption correction, SIR-92[83] and SHELXL-97[84] for structure solution, and SHELXL[84] as well as ShelXle[85] for structure refinement. The hydrogen atoms were placed in idealized positions and constrained to ride on their parent atom. The positions of the hydrogen atoms in the OH groups were found with a difference Fourier analysis of the remaining electron density. The last cycles of refinement included atomic positions for all atoms, anisotropic thermal parameters for all non-hydrogen atoms, and isotropic thermal parameters for all hydrogen atoms.

Scheme 8. Numbering for the Ligands Used Throughout the Experimental Section[a]

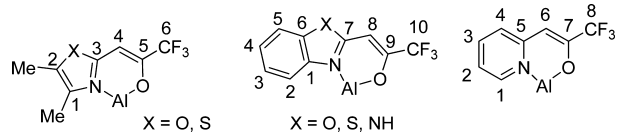

[a]In the octahedral complexes with three magnetically unequivalent ligands the corresponding ligand signals are named *mer*-a, *mer*-b, and *mer*-c.

General Procedure for the Synthesis of $Al(O^{\wedge}N)_3$ and $MeAl(O^{\wedge}N)_2$ Complexes. To a stirred solution of 1 equiv of $AlMe_3$ (1.0 M solution in heptane) in 5 mL of toluene cooled to −78 °C, a solution of 2 or 3 equiv of the appropriate chelate ligand, dissolved in 5 mL of toluene, was added dropwise. The reaction mixture was allowed to warm to ambient temperature and was stirred for 24 h. All volatiles were removed under reduced pressure. Excess of the ligand was removed either by sublimation or by washing the raw product with dimethyl sulfoxide (DMSO).

Al(DMOTFP)$_3$. Yield: 87%, *fac*/*mer* ratio: 1:99. ^1H NMR (300 MHz, 298 K, acetone-d_6): δ (ppm) = 6.12 (s, H4, *mer*-a), 5.91 (s, H4, *mer*-b), 5.76 (s, H4, *mer*-c), 2.31 (s, Me-2, *mer*-c), 2.27 (s, Me-2, *mer*-b), 2.20 (s, Me-2, *mer*-a), 1.85 (s, Me-1, *mer*-c), 1.75 (s, Me-1, *mer*-b), 1.47 (s, Me-1, *mer*-a). $^{13}C\{^1H\}$ NMR (75 MHz, 298 K, acetone-d_6): δ (ppm) = 162.3 (C3, *mer*-b and *mer*-c), 161.7 (C3, *mer*-a), 157.8 (C5, *mer*-c), 157.3 (C5, *mer*-b), 155.7 (C5, *mer*-a), 143.2 (C1, *mer*-c), 142.3 (C1, *mer*-b), 141.2 (C1, *mer*-a), 128.5 (C2, *mer*-c), 127.6 (C2, *mer*-b), 127.1 (C2, *mer*-a), 120.1 (C6, *mer*-c and *mer*-a), 119.6 (C6, *mer*-b), 85.6 (C4, *mer*-a), 84.5 (C4, *mer*-b), 84.0 (C4, *mer*-c), 8.9 (Me-1, *mer*-c), 8.6 (Me-1, *mer*-b; Me-2, *mer*-b; Me-2, *mer*-c and Me-2, *mer*-a), 8.3 (Me-1, *mer*-a). ^{19}F NMR (282 MHz, 298 K, acetone-d_6): δ (ppm) = −75.7 (s, *mer*-a and *mer*-c), −75.2 (s, *mer*-b). ^{27}Al NMR (104 MHz, 298 K, acetone-d_6): δ (ppm) = 8 ($\Delta_{1/2}$ = 700 Hz). EI-MS: 645 (12, M^+), 458 (4, $Al(DMOTFP)_2F^+$), 439 (100, $Al(DMOTFP)_2^+$), 168 (4,

dx.doi.org/10.1021/ic502549m | Inorg. Chem. 2015, 54, 25−37

$C_8H_7FNO_2^+$). Elem. Anal. found: C 44.75, H 3.63, N 6.73, calc. for $(C_8H_7NO_2F_3)_3Al$: C 44.66, H 3.28, N 6.51%.

Al(PyTFP)$_3$. Yield: 90%, *fac*/*mer* ratio: 25:75. ^{1}H NMR (400 MHz, 203 K, acetone-d_6): δ (ppm) = 8.44 (m, H1, *mer*-a and *mer*-c), 8.29 (d, H1, *fac*), 8.07 (t, H3, *mer*-c), 8.01 (t, H3, *mer*-a), 7.91 (t, H3, *mer*-b), 7.62 (d, H4, *mer*-a), 7.59 (m, H3, *fac*), 7.55 (d, H4, *mer*-c), 7.50 (m, H2, *mer*-c), 7.49 (m, H4, *mer*-b), 7.42 (d, H1, *mer*-b), 7.37 (t, H2, *mer*-a), 7.21 (d, H4, *fac*), 7.13 (t, H2, *mer*-b), 6.64 (t, H2, *fac*), 6.35 (s, H6, *mer*-a), 6.09 (s, H6, *mer*-b), 6.07 (s, H6, *mer*-c), 5.98 (s, H6, *fac*). ^{13}C{^{1}H} NMR (100 MHz, 203 K, acetone-d_6): δ (ppm) = 157 (C5, *mer*-b), 155 (C5, *mer*-c), 154 (C5, *mer*-a and C7, *mer*-b), 153 (C7, *mer*-c), 152 (C7, *mer*-a and *fac*), 148.7 (C1, *mer*-a), 148.6 (C5, *fac*), 148.1 (C1, *mer*-c), 147.1 (C1, *mer*-b), 141.1 (C3, *mer*-c), 140.4 (C3, *mer*-a), 137.9 (C3, *mer*-b), 137.8 (C3, *fac*), 125.0 (C4, *mer*-c), 124.8 (C4, *mer*-a), 124.0 (C2, *mer*-c), 123.7 (C4, *mer*-b and *fac*), 120.7 (C2 and C8, *mer*-a), 120.6 (C8, *fac*), 120.5 (C8, *mer*-b), 120.1 (C8, *mer*-c), 119.6 (C2, *mer*-b), 119.2 (C2, *fac*), 97.1 (C6, *mer*-a), 96.5 (C6, *fac*), 96.3 (C6, *mer*-c), 96.1 (C6, *mer*-b). ^{19}F NMR (377 MHz, 203 K, acetone-d_6): δ (ppm) = −74.7 (*mer*-a), −74.6 (*fac*), −74.5 (*mer*-b), −74.3 (*mer*-c). ^{27}Al NMR (78 MHz, 298 K, acetone-d_6): δ (ppm) = 9 ($\Delta_{1/2}$ = 1500 Hz). EI-MS: 591 (16, M$^+$), 422 (4, Al(PyTFP)$_2$F$^+$), 403 (100, Al(PyTFP)$_2^+$), 189 (6, PyTFP$^+$), 150 (16, PyTFP$^+$ −2F), 120 (4, PyTFP$^+$ −CF$_3$). Elem. Anal. found: C 48.58, H 3.02, N 6.68; calc. for $(C_8H_5NOF_3)_3Al$: C 48.72, H 2.56, N 7.11; calc. for $[(C_8H_5NOF_3)_2AlOH]_2$: C 45.73, H 2.64, N 6.67%.

Al(BITFP)$_3$. Yield: 82%, *fac*/*mer* ratio: 20:80. ^{1}H NMR (600 MHz, 298 K, chloroform-d_1): δ (ppm) = 12.08 (s, NH, *mer*-c), 12.07 (s, NH, *mer*-a), 11.69 (s, NH, *mer*-b), 10.28 (s, NH, *fac*), 8.01 (d, H2, *fac*), 7.54 (d, H2, *mer*-c), 7.52 (d, H5, *mer*-c), 7.44 (d, H5, *mer*-a), 7.39 (d, H5, *mer*-b), 7.37 (d, H2, *mer*-a), 7.22 (m, H4, *mer*-c), 7.14 (m, H4, *fac*), 7.10 (m, H3, *mer*-c and H4, *mer*-a), 7.09 (m, H3, *fac*), 7.02 (m, H4, *mer*-b), 7.00 (m, H5, *fac*), 6.98 (m, H3, *mer*-a), 6.57 (t, H3, *mer*-b), 6.46 (s, H8, *mer*-c), 5.98 (d, H2, *mer*-b), 5.96 (s, H8, *mer*-b), 5.83 (s, H8, *mer*-a), 5.72 (s, H8, *fac*). ^{13}C{^{1}H} NMR (150 MHz, 298 K, chloroform-d_1): δ (ppm) = 158.2 (C9, *mer*-b), 157.6 (C9, *mer*-a), 156.8 (C9, *mer*-c), 156.6 (C9, *fac*), 153.6 (C7, *mer*-b), 153.3 (C7, *mer*-a), 152.8 (C7, *mer*-c), 151.7 (C7, *fac*), 140.0 (C1, *mer*-b), 139.3 (C1, *mer*-c), 139.1 (C1, *mer*-a), 138.1 (C1, *fac*), 132.5 (C6, *mer*-c), 132.2 (C6, *mer*-a and C4, *mer*-c), 131.9 (C6, *fac*), 131.6 (C6, *mer*-b), 125.4 (C4, *fac*), 122.9 (C3, *mer*-c), 122.6 (C4, *mer*-a), 122.3 (C3, *mer*-a), 122.0 (C3, *fac*), 121.9 (C4, *mer*-b), 121.8 (C3, *mer*-b), 120.7 (C10, *fac*), 120.5 (C10, *mer*-b), 120.4 (C10, *mer*-c), 120.3 (C10, *mer*-a), 119.2 (C2, *fac*), 117.2 (C2, *mer*-c), 117.1 (C2, *mer*-a), 115.2 (C2, *mer*-b), 111.1 (C5, *mer*-c), 110.8 (C5, *mer*-a), 110.6 (C5, *mer*-b), 109.5 (C5, *fac*), 86.5 (C8, *mer*-c), 85.6 (C8, *mer*-a), 85.4 (C8, *fac*), 84.7 (C8, *mer*-b). ^{19}F NMR (282 MHz, 298 K, chloroform-d_1): δ (ppm) = −75.2 (*mer*-c), −75.0 (*mer*-b), −74.7 (*mer*-a), −73.9 (*fac*). ^{27}Al NMR (104 MHz, 298 K, acetone-d_6): δ (ppm) = 7 ($\Delta_{1/2}$ = 400 Hz). EI-MS: 708 (4, M$^+$), 518 (12, Al(BITFP)$_2$F$_2^+$), 500 (100, Al(BITFP)$_2$F$^+$), 481 (44, Al(BITFP)$_2^+$), 431 (12, Al(BITFP)$_2$F$^+$ −CF$_3$), 292 (4, Al(BITFP)-F$_2^+$), 228 (48, BITFP$^+$), 208 (12, BITFP$^+$-F), 159 (28, BITFP$^+$ −CF$_3$), 131 (8, BITFP$^+$ −COCF$_3$). Elem. Anal. found: C 50.53, H 2.35, N 11.52; calc. for $(C_{10}H_6N_2OF_3)_3Al$: C 50.86, H 2.56, N 11.86%.

Al(BOTFP)$_3$. Yield: 89%, *fac*/*mer* ratio: 25:75. ^{1}H NMR (600 MHz, 298 K, chloroform-d_1): δ (ppm) = 7.54 (m, H5, *mer*-a), 7.51 (m, H5, *mer*-b), 7.46 (m, H5, *mer*-c), 7.45 (m, H2, *mer*-a), 7.42 (m, H4, *mer*-a), 7.40 (m, H3, *mer*-a), 7.36 (m, H2, *fac*), 7.32 (m, H2, *mer*-b, H3 and H4, *fac*), 7.30 (m, H4, *mer*-b), 7.24 (t, H3, *mer*-b), 7.18 (t, H4, *mer*-c), 7.08 (m, H5, *fac*), 6.83 (t, H3, *mer*-c), 6.45 (s, H8, *mer*-b), 6.04 (d, H2, *mer*-c), 6.05 (s, H8, *mer*-c), 5.90 (s, H8, *mer*-a), 5.84 (s, H8, *fac*). ^{13}C{^{1}H} NMR (150 MHz, 298 K, chloroform-d_1): δ (ppm) = 167.1 (C7, *mer*-c), 166.9 (C7, *mer*-a), 166.4 (C7, *mer*-b), 165.2 (C7, *fac*), 163.6 (C9, *mer*-c), 162.8 (C9, *mer*-a), 161.5 (C9, *fac*), 161.4 (C9, *mer*-b), 148.3 (C6, *mer*-a and C6, *mer*-b), 147.8 (C6, *mer*-c and *fac*), 137.1 (C1, *mer*-c), 136.4 (C1, *mer*-a), 136.0 (C1, *mer*-b), 135.2 (C1, *fac*), 126.2 (C3, *mer*-a), 125.8 (C4, *mer*-a), 125.6 (C3, *mer*-b), 125.2 (C4, *mer*-b and C3, *mer*-c), 124.9 (C3, *fac*), 124.8 (C4, *fac*), 124.4 (C4, *mer*-c), 119.3 (C10, *mer*-b), 119.2 (C10, *mer*-c and *fac*), 119.0 (C10, *mer*-a), 117.7 (C2, *mer*-a), 117.6 (C2, *mer*-b), 117.2 (C2, *fac*), 114.7 (C2, *mer*-c), 110.8 (C5, *mer*-a and C5, *mer*-c), 110.6 (C5, *mer*-b), 110.1 (C5, *fac*), 85.9 (C8, *mer*-b), 84.8 (C8, *mer*-a), 84.3 (C8, *fac*), 83.9 (C8, *mer*-c). ^{19}F NMR (282 MHz, 298 K, chloroform-d_1): δ (ppm) = −75.5 (*mer*-c), −75.4 (*mer*-b), −75.0 (*mer*-a), −74.3 (*fac*). ^{27}Al NMR (104 MHz, 298 K, acetone-d_6): δ (ppm) = 9 ($\Delta_{1/2}$ = 700 Hz). EI-MS: 711 (20, M$^+$), 483 (100, Al(BOTFP)$_2^+$), 190 (4, BOTFP$^+$ −2F). Elem. Anal. found: C 50.12, H 2.33, N 5.55; calc. for $(C_{10}H_6NO_2F_3)_3Al$: C 50.65, H 2.13, N 5.91; calc. for $[(C_{10}H_6NO_2F_3)_2AlOH]_2$: C 48.02, H 2.22, N 5.60%.

MeAl(DMTTFP)$_2$. Yield: 80%. ^{1}H NMR (300 MHz, 298 K, acetone-d_6): δ (ppm) = 6.43 (s, H4, 1H), 2.48 (s, Me-1, 3H), 2.44 (s, Me-2, 3H), −0.71 (s, Al-C**H**$_3$, 3H). ^{13}C{^{1}H} NMR (75 MHz, 298 K, acetone-d_6): δ (ppm) = 162.3 (C3), 149.5 (C5), 146.9 (C1), 125.4 (C2), 120.3 (C6), 93.5 (C4), 13.2 (Me-1), 10.4 (Me-2), −3.6 (Al-**C**H$_3$). ^{19}F NMR (282 MHz, 298 K, acetone-d_6): δ (ppm) = −74.1 ($^1J_{C,F}$ = 277 Hz, $^2J_{C,F}$ = 34 Hz). ^{27}Al NMR (78 MHz, 298 K, acetone-d_6): δ (ppm) = 13 ($\Delta_{1/2}$ = 4000 Hz). EI-MS: 471 (100, Al(DMTTFP)$_2^+$), 223 (12, DMTTFP$^+$), 184 (14, DMTTFP$^+$ −2F), 154 (12, DMTTFP$^+$ −CF$_3$). Elem. Anal. found: C 41.12, H 3.51, N 5.72, S 13.62; calc. for $(C_8H_7NOSF_3)_2AlCH_3$: C 41.98, H 3.52, N 5.55, S 13.18; calc. for $[(C_8H_7NOSF_3)_2Al]_2O$: C 40.09, H 2.94, N 5.84, S 13.38%.

MeAl(BTTFP)$_2$. Yield: 84%. ^{1}H NMR (300 MHz, 298 K, acetone-d_6): δ (ppm) = 8.22 (d, H2, 1H), 7.85 (d, H5, 1H), 7.54 (t, H3, 1H), 7.45 (t, H4, 1H), 6.35 (s, H8, 1H), −0.57 (s, Al-CH$_3$, 3H). ^{13}C{^{1}H} NMR (75 MHz, 298 K, acetone-d_6): δ (ppm) = 167.4 (C7), 154.7 (C9), 149.2 (C1), 130.8 (C6), 126.7 (C3), 125.7 (C4), 122.4 (C2), 121.1 (C5), 119.2 (C10), 93.7 (C8), −6.2 (Al-CH$_3$). ^{19}F NMR (282 MHz, 298 K, acetone-d_6): δ (ppm) = −74.1 ($^1J_{C,F}$ = 279 Hz, $^2J_{C,F}$ = 35 Hz). ^{27}Al NMR (78 MHz, 298 K, acetone-d_6): δ (ppm) = 10 ($\Delta_{1/2}$ = 5000 Hz). EI-MS: 515 (100, Al(BTTFP)$_2^+$), 245 (4, BTTFP$^+$), 206 (12, BTTFP$^+$ −2F), 178 (8, BTTFP$^+$ −CF$_3$). Elem. Anal. found: C 47.81, H 2.40, N 5.88, S 12.00; calc. for $(C_{10}H_6NOSF_3)_2AlCH_3$: C 47.55, H 2.47, N 5.28, S 12.09%.

[Al(BOTFP)$_2$OH]$_2$. ^{1}H NMR (300 MHz, 298 K, acetone-d_6): δ (ppm) = 8.10 (m, H2, 1H), 7.31 (m, H3 and H4, 2H), 7.13 (m, H5, 1H), 5.90 (s, H8, 1H), 3.69 (s broad, OH). ^{13}C{^{1}H} NMR (75 MHz, 298 K, acetone-d_6): δ (ppm) = 164.9 (C7), 161.7 (C9), 147.5 (C6), 135.8 (C1), 124.4 (C3 and C4), 119.7 (C10), 118.4 (C2), 109.6 (C5), 83.3 (C8). ^{19}F NMR (282 MHz, 298 K, acetone-d_6): δ (ppm) = −74.8 ($^2J_{C,F}$ = 34 Hz). EI-MS: 982 (28, Al$_2$(BOTFP)$_4$O$^+$), 754 (36, Al$_2$(BOTFP)$_3$O$^+$), 711 (20, Al(BOTFP)$_3^+$), 502 (4, Al(BOTFP)$_2$F$^+$), 483 (100, Al(BOTFP)$_2^+$), 433 (8, Al(BOTFP)$_2$F$^+$ −CF$_3$), 18 (40, H$_2$O).

General Procedure for the Synthesis of Al(BTTFP)$_3$ and Al(DMTTFP)$_3$. To a stirred solution of 1 equiv of $[Al(O^tBu)_3]_2$ in 20 mL of toluene, 6 equiv of the ligand were added. This suspension was stirred for 6 h at ambient temperature. Solvent was removed under reduced pressure, and unreacted $[Al(O^tBu)_3]_2$ was removed by sublimation (10^{-3} mbar).

Al(DMTTFP)$_3$. Yield: 86%, *fac*/*mer* ratio: 5:95. ^{1}H NMR (300 MHz, 298 K, benzene-d_6): δ (ppm) = 6.28 (s, 4H, *mer*), 6.26 (s, 4H, *mer*), 6.11 (s, 4H, *mer*), 5.86 (s, 4H, *fac*), 2.03 (s, Me, *mer*), 1.98 (s, Me, *mer*), 1.90 (s, Me, *mer*), 1.69 (s, Me, *mer*), 1.48 (s, Me, *mer*), 1.41 (s, Me, *mer*). ^{13}C{^{1}H} NMR (75 MHz, 298 K, benzene-d_6): δ (ppm) = 166.2 (C3, *mer*), 164.8 (C3, *mer*), 162.5 (C3, *mer*), 153.0 (C5, *mer*), 151.4 (C5, *mer*), 149.4 (C5, *mer*), 148.8 (C2, *mer*), 147.6 (C2, *mer*), 146.8 (C2, *mer*), 124.4 (C1, *mer*), 124.3 (C1, *mer*), 123.8 (C1, *mer*), 120.9 (C6, *mer*), 120.8 (2 × C6, *mer*), 97.9 (C4, *mer*), 94.7 (C4, *mer*), 93.9 (C4, *mer*), 14.4 (Me, *mer*), 13.9 (Me, *mer*), 12.9 (Me, *mer*),11.0 (Me, *mer*), 10.9 (Me, *mer*), 10.8 (Me, *mer*). ^{19}F NMR (282 MHz, 298 K, benzene-d_6) δ (ppm) = −72.0 (*mer*), −73.3 (*fac*), −73.7 (*mer*), −73.8 (*mer*). ^{27}Al NMR (78 MHz, 298 K, benzene-d$_6$): δ (ppm) = 17 ($\Delta_{1/2}$ = 5000 Hz).

EI-MS: 584 (4, M$^+$ −CF$_3$), 490 (4, (DMTTFP)$_2$AlF$^+$), 471 (100, Al(DMTTFP)$_2^+$), 223 (4, DMTTFP$^+$), 184 (4, DMTTFP$^+$ −2F), 154 (4, DMTTFP$^+$ −CF$_3$).

Al(BTTFP)$_3$. ^{1}H NMR (300 MHz, 298 K, benzene-d_6): δ (ppm) = 7.73 (d, *mer*), 7.50 (d, *mer*), 7.02−6.71 (m, *mer*), 6.59 (m, *mer*), 6.41 (t, *mer*), 6.26 (s, *mer*), 5.62 (s, *mer*). ^{19}F NMR (282 MHz, 298 K,

dx.doi.org/10.1021/ic502549m | *Inorg. Chem.* 2015, 54, 25−37

benzene-d_6): δ (ppm) = −74.5 (*mer*), −74.4 (*mer*), −73.2 (*mer*). ^{27}Al NMR (104 MHz, 298 K, acetone-d_6): δ (ppm) = 9 ($\Delta_{1/2}$ = 700 Hz).

EI-MS: 758, (4, M^+), 534, (100, $(BTTFP)_2AlF^+$), 515 (100, $(BTTFP)_2Al^+$), 245 (10, $BTTFP^+$), 206 (4, $BTTFP^+$ −2F), 176 (8, $BTTFP^+$ $-CF_3$).

[Al(H-PyTFP)(O^{t}Bu)$_2$]$_2$. To a stirred solution of 2 equiv of H-PyTFP in 20 mL of toluene a solution of 1 equiv of $[Al(O^tBu)_3]_2$ in 20 mL of toluene was added. The reaction mixture was stirred for 6 h at ambient temperatures. All volatiles were removed under reduced pressure. Excess ligand was removed by sublimation, and the product was further purified by sublimation.

Yield: 75%.^{1}H NMR (300 MHz, 298 K, benzene-d_6): δ (ppm) = 9.82 (d, H1, 1H), 7.01 (t, H3, 1H), 6.85 (t, H2, 1H), 6.54 (d, H4, 1H), 6.15 (s, H6, 1H), 1.58 (s, terminal CH_3, 9H), 1.43 (s, bridging CH_3, 9H). $^{13}C\{^1H\}$ NMR (75 MHz, 298 K, benzene-d_6): δ (ppm) = 156.2 (C5), 153.0 (C7), 149.3 (C1), 138.0 (C3), 123.7 (C4), 121.4 (C8), 118.7 (C2), 98.1 (C6), 76.2 (C_q, bridging), 69.5 (C_q, terminal), 34.0 (CH_3, terminal), 30.9 (CH_3, bridging). ^{19}F NMR (282 MHz, 298 K, benzene-d_6): δ (ppm) = −73.6. ^{27}Al NMR (282 MHz, 298 K, benzene-d_6): δ (ppm) = 45 (Al_{tetra}, $\Delta_{1/2}$ = 2000 Hz), 8 (Al_{octa}, $\Delta_{1/2}$ = 1000 Hz). EI-MS: 707 (12, $[Al(PyTFP)(O^tBu)_2]_2^+$ $-CH_3$), 593 (20, $[Al(PyTFP)(O^tBu)_2]_2^+$ $-CH_3$, −2 $C(CH_3)_3$), 577 (16, $[Al(PyTFP)(O^tBu)_2]_2^+$ −2 CH_3, −2 $C(CH_3)_3$), 534 (100, $[Al(PyTFP)(O^tBu)_2]_2^+$ -PyTFP), 519 (34, $[Al(PyTFP)(O^tBu)_2]_2^+$ -PyTFP, $-CH_3$), 478 (10, $[Al(PyTFP)(O^tBu)_2]_2^+$ -PyTFP, $-C(CH_3)_3$), 422 (8, $[Al(PyTFP)(O^tBu)_2]_2^+$ -PyTFP, −2 $C(CH_3)_3$), 403 (6, $[Al(PyTFP)(O^tBu)_2]_2^+$ -PyTFP, −2 $C(CH_3)_3$, -F), 366 (10, $[Al(PyTFP)(O^tBu)_2]_2^+$ -PyTFP, −3 $C(CH_3)_3$), 310 (6, $[Al(PyTFP)(O^tBu)_2]_2^+$ -PyTFP, −4 $C(CH_3)_3$). Elem. Anal. calc. for $(C_8H_5NOF_3)_2Al_2(OC(CH_3)_3)_4$: C 53.18, H 6.42, N 3.88, found: C 52.23, H 7.14, N 4.05%.

■ ASSOCIATED CONTENT

Supporting Information

X-ray crystallographic data files (CCDC 956240−956245) in CIF format, synthesis and analysis of H-BTTFP, including selected crystallographic data and collection parameters, and drawings of H-BTTFP indicating atom labeling scheme and intermolecular hydrogen-bonding arrangement of neighboring H-BTTFP molecules. This material is available free of charge via the Internet at http://pubs.acs.org.

■ AUTHOR INFORMATION

Corresponding Author

*E-mail: sanjay.mathur@uni-koeln.de.

Notes

The authors declare no competing financial interest.

■ ACKNOWLEDGMENTS

The authors gratefully acknowledge the University of Cologne and the Regional Research Cluster Sustainable Chemical Synthesis for financial support. The project "Sustainable Chemical Synthesis (SusChemSys)" is cofinanced by the European Regional Development Fund (ERDF) and the state of North Rhine-Westphalia, Germany, under the Operational Programme "Regional Competitiveness and Employment" 2007−2013.

■ REFERENCES

(1) Altmayer, J.; Barth, S.; Mathur, S. *RSC Adv.* **2013**, *3*, 11234−11239.
(2) Müller, R.; Hernandez-Ramirez, F.; Shen, H.; Du, H.; Mader, W.; Mathur, S. *Chem. Mater.* **2012**, *24*, 4028−4035.
(3) Llauro, G.; Hillel, R.; Sibieude, F. *Chem. Vap. Deposition* **1998**, *4*, 247−252.
(4) Hasenkox, U.; Hoffmann, S.; Waser, R. *J. Sol-Gel Sci. Technol.* **1998**, *12*, 67−79.
(5) de Kroon, A. P.; Schaefer, G. W.; Aldinger, F. *Chem. Mater.* **1995**, *7*, 878−887.
(6) Fortman, J. J.; Sievers, R. E. *Inorg. Chem.* **1967**, *6*, 2022−2029.
(7) Kroll, W. R.; Naegele, W. *J. Organomet. Chem.* **1969**, *19*, 439−443.
(8) Hon, P. K.; Pfluger, C. E. *J. Coord. Chem.* **1973**, *3*, 67−76.
(9) Morris, M. L.; Koob, R. D. *Inorg. Chem.* **1981**, *20*, 2737−2738.
(10) Umecky, T.; Kanakubo, M.; Ikushima, Y. *J. Phys. Chem. B* **2011**, *115*, 10622−10630.
(11) Smolentsev, A. I.; Zherikova, K. V.; Trusov, M. S.; Stabnikov, P. A.; Naumov, D. Y.; Borisov, S. V. *J. Struct. Chem.* **2011**, *52*, 1070−1077.
(12) Hemmer, E.; Huch, V.; Adlung, M.; Wickleder, C.; Mathur, S. *Eur. J. Inorg. Chem.* **2011**, 2148−2157.
(13) Mathur, S.; Veith, M.; Ruegamer, T.; Hemmer, E.; Shen, H. *Chem. Mater.* **2004**, *16*, 1304−1312.
(14) Moravec, Z.; Sluka, R.; Necas, M.; Jancik, V.; Pinkas, J. *Inorg. Chem.* **2009**, *48*, 8106−8114.
(15) Lin, C.-Y.; Lee, H. M.; Huang, J.-H. *J. Organomet. Chem.* **2007**, *692*, 3718−3722.
(16) Mehrotra, R. C. *J. Indian Chem. Soc.* **1953**, *30*, 585−591.
(17) Shiner, V. J.; Whittaker, D.; Fernande, V. P. *J. Am. Chem. Soc.* **1963**, *85*, 2318−&.
(18) Buining, P. A.; Pathmamanoharan, C.; Jansen, J. B. H.; Lekkerkerker, H. N. W. *J. Am. Ceram. Soc.* **1991**, *74*, 1303−1307.
(19) Kuzminykh, Y.; Dabirian, A.; Reinke, M.; Hoffmann, P. *Surf. Coat. Technol.* **2013**, *230*, 13−21.
(20) Battiston, G. A.; Carta, G.; Cavinato, G.; Gerbasi, R.; Porchia, M.; Rossetto, G. *Chem. Vap. Deposition* **2001**, *7*, 69−74.
(21) Blittersdorf, S.; Bahlawane, N.; Kohse-Höinghaus, K.; Atakan, B.; Müller, J. *Chem. Vap. Deposition* **2003**, *9*, 194−198.
(22) Glass, J. A.; Kher, S. S.; Spencer, J. T. *Chem. Mater.* **1992**, *4*, 530−538.
(23) Dumitrescu, L.; Maury, F. *Surf. Coat. Technol.* **2000**, *125*, 419−423.
(24) Ito, A.; Tu, R.; Goto, T. *Surf. Coat. Technol.* **2010**, *204*, 2170−2174.
(25) Pflitsch, C.; Muhsin, A.; Bergmann, U.; Atakan, B. *Surf. Coat. Technol.* **2006**, *201*, 73−81.
(26) Singh, M. P.; Shivashankar, S. A. *Surf. Coat. Technol.* **2002**, *161*, 135−143.
(27) Giebelhaus, I.; Müller, R.; Tyrra, W.; Pantenburg, I.; Fischer, T.; Mathur, S. *Inorg. Chim. Acta* **2011**, *372*, 340−346.
(28) Brückmann, L.; Tyrra, W.; Stucky, S.; Mathur, S. *Inorg. Chem.* **2012**, *51*, 536−542.
(29) Appel, L.; Fiz, R.; Tyrra, W.; Mathur, S. *Dalton Trans.* **2012**, *41*, 1981−1990.
(30) Mathur, S.; Shen, H.; Donia, N. *ECS Trans.* **2006**, *3*, 3−13.
(31) McGrath, T. F.; Levine, R. *J. Am. Chem. Soc.* **1955**, *77*, 3656−3658.
(32) Root, C. A.; Rowe, J. E.; Veening, H. *Inorg. Chem.* **1971**, *10*, 1195−1197.
(33) Narsaiah, B.; Sivaprasad, A.; Venkataratnam, R. V. *J. Fluorine Chem.* **1994**, *66*, 47−50.
(34) Meazza, G.; Paravidino, P.; Bettarini, F.; Forgia, D.; Fornara, L. Derivatives of 1,3-Diones Having a Herbicidal Activity; Patent WO2005030736 A1, 2005.
(35) Wolleb, H.; Wolleb, A.; Bienewald, F.; Schmidhalter, B.; Budry, J.-L. Metal Chelates and Their Use in Optical Recording Media Having High Storage Capacity; Patent US20080193700 A1, 2005.
(36) Chandra Sheker Reddy, A.; Shanthan Rao, P.; Venkataratnam, R. V. *Tetrahedron* **1997**, *53*, 5847−5854.
(37) Wigton, F. B.; Joullié, M. M. *J. Am. Chem. Soc.* **1959**, *81*, 5212−5215.
(38) Kawase, M.; Teshima, M.; Saito, S.; Tani, S. *Heterocycles* **1998**, *48*, 2103−2109.
(39) Veith, M.; Kneip, S. J.; Jungmann, A.; Hüfner, S. *Z. Anorg. Allg. Chem.* **1997**, *623*, 1507−1517.
(40) Szigethy, G.; Heyduk, A. F. *Dalton Trans.* **2012**, *41*, 8144−8152.

(41) Roesky, H. W. *Inorg. Chem.* **2004**, *43*, 7284−7293.
(42) Nagendran, S.; Roesky, H. W. *Organometallics* **2008**, *27*, 457−492.
(43) Myers, T. W.; Kazem, N.; Stoll, S.; Britt, R. D.; Shanmugam, M.; Berben, L. A. *J. Am. Chem. Soc.* **2011**, *133*, 8662−8672.
(44) Yang, Z.; Zhu, H.; Ma, X.; Chai, J.; Roesky, H. W.; He, C.; Magull, J.; Schmidt, H.-G.; Noltemeyer, M. *Inorg. Chem.* **2006**, *45*, 1823−1827.
(45) Yang, Y.; Li, H.; Wang, C.; Roesky, H. W. *Inorg. Chem.* **2012**, *51*, 2204−2211.
(46) Yang, Z.; Hao, P.; Liu, Z.; Ma, X.; Roesky, H. W.; Yang, Y.; Li, J. *Z. Anorg. Allg. Chem.* **2013**, *639*, 2618−2622.
(47) Myers, T. W.; Berben, L. A. *Inorg. Chem.* **2012**, *51*, 1480−1488.
(48) Myers, T. W.; Holmes, A. L.; Berben, L. A. *Inorg. Chem.* **2012**, *51*, 8997−9004.
(49) Fedushkin, I. L.; Moskalev, M. V.; Baranov, E. V.; Abakumov, G. A. *J. Organomet. Chem.* **2013**, *747*, 235−240.
(50) Fedushkin, I. L.; Lukoyanov, A. N.; Hummert, M.; Schumann, H. *Z. Anorg. Allg. Chem.* **2008**, *634*, 357−361.
(51) Lukoyanov, A. N.; Fedushkin, I. L.; Schumann, H.; Hummert, M. *Z. Anorg. Allg. Chem.* **2006**, *632*, 1471−1476.
(52) Bouyahyi, M.; Roisnel, T.; Carpentier, J.-F. *Organometallics* **2010**, *29*, 491−500.
(53) Li, C.-Y.; Tsai, C.-Y.; Lin, C.-H.; Ko, B.-T. *Dalton Trans.* **2011**, *40*, 1880−1887.
(54) Qiao, S.; Ma, W.-A.; Wang, Z.-X. *J. Organomet. Chem.* **2011**, *696*, 2746−2753.
(55) Bertolasi, V.; Gilli, P.; Ferretti, V.; Gilli, G. *Acta Crystallogr., Sect. B* **1995**, *51*, 1004−1015.
(56) Gilli, P.; Bertolasi, V.; Ferretti, V.; Gilli, G. *J. Am. Chem. Soc.* **2000**, *122*, 10405−10417.
(57) Hoveyda, H. R.; Rettig, S. J.; Orvig, C. *Inorg. Chem.* **1993**, *32*, 4909−4913.
(58) Li, W.; Olmstead, M. M.; Miggins, D.; Fish, R. H. *Inorg. Chem.* **1996**, *35*, 51−55.
(59) Yang, Y.; Schulz, T.; John, M.; Yang, Z.; Jiménez-Pérez, V. M.; Roesky, H. W.; Gurubasavaraj, P. M.; Stalke, D.; Ye, H. *Organometallics* **2008**, *27*, 769−777.
(60) Das, M.; Haworth, D. T.; Beery, J. W. *Inorg. Chim. Acta* **1981**, *49*, 17−20.
(61) Saito, K.; Nagasawa, A. *Polyhedron* **1990**, *9*, 215−222.
(62) Mathur, S.; Veith, M.; Haas, M.; Shen, H.; Lecerf, N.; Huch, V.; Hüfner, S.; Haberkorn, R.; Beck, H. P.; Jilavi, M. *J. Am. Chem. Soc.* **2001**, *84*, 1921−1928.
(63) Veith, M.; Mathur, S.; Mathur, C. *Polyhedron* **1998**, *17*, 1005−1034.
(64) Benn, R.; Janssen, E.; Lehmkuhl, H.; Rufinska, A. *J. Organomet. Chem.* **1987**, *333*, 155−168.
(65) Benn, R.; Rufinska, A. *Angew. Chem., Int. Ed.* **1986**, *25*, 861−881.
(66) König, R.; Scholz, G.; Thong, N. H.; Kemnitz, E. *Chem. Mater.* **2007**, *19*, 2229−2237.
(67) Akitt, J. W. *Prog. Nucl. Magn. Reson. Spectrosc.* **1989**, *21*, 1−149.
(68) Florczak, M.; Kowalski, A.; Libiszowski, J.; Majerska, K.; Duda, A. *Polimery* **2007**, *52*, 722−729.
(69) Sharma, N.; Sharma, R. K.; Bohra, R.; Drake, J. E.; Hursthouse, M. B.; Light, M. E. *J. Chem. Soc., Dalton Trans.* **2002**, 1631−1634.
(70) Brückmann, L.; Tyrra, W.; Mathur, S.; Berden, G.; Oomens, J.; Meijer, A. J. H. M.; Schäfer, M. *ChemPhysChem* **2012**, *13*, 2037−2045.
(71) Rutherford, D.; Atwood, D. A. *Organometallics* **1996**, *15*, 4417−4422.
(72) Wang, Y.; Bhandari, S.; Prakin, S.; Atwood, D. A. *J. Organomet. Chem.* **2004**, *689*, 759−765.
(73) Lee, J.; Kim, S. H.; Lee, K. M.; Hwang, K. Y.; Kim, H.; Huh, J. O.; Kim, D. J.; Lee, Y. S.; Do, Y.; Kim, Y. *Organometallics* **2010**, *29*, 347−353.
(74) Addison, A. W.; Rao, T. N.; Reedijk, J.; van Rijn, J.; Verschoor, G. C. *J. Chem. Soc., Dalton Trans.* **1984**, 1349−1356.
(75) Gurian, P. L.; Cheatham, L. K.; Ziller, J. W.; Barron, A. R. *J. Chem. Soc., Dalton Trans.* **1991**, 1449−1456.
(76) Liao, S.-H.; Shiu, J.-R.; Liu, S.-W.; Yeh, S.-J.; Chen, Y.-H.; Chen, C.-T.; Chow, T. J.; Wu, C.-I. *J. Am. Chem. Soc.* **2009**, *131*, 763−777.
(77) Brinkmann, M.; Gadret, G.; Muccini, M.; Taliani, C.; Masciocchi, N.; Sironi, A. *J. Am. Chem. Soc.* **2000**, *122*, 5147−5157.
(78) Wengrovius, J. H.; Garbauskas, M. F.; Williams, E. A.; Going, R. C.; Donahue, P. E.; Smith, J. F. *J. Am. Chem. Soc.* **1986**, *108*, 982−989.
(79) Garbauskas, M. F.; Wengrovius, J. H.; Going, R. C.; Kasper, J. S. *Acta Crystallogr., Sect. C: Cryst. Struct. Commun.* **1984**, *C40*, 1536−1540.
(80) Lichtenberger, R.; Puchberger, M.; Baumann, S. O.; Schubert, U. *J. Sol-Gel Sci. Technol.* **2009**, *50*, 130−140.
(81) *STOE X-RED32, Data Reduction Program;* Stoe & Cie GmbH: Darmstadt, Germany, 2002.
(82) *STOE X-SHAPE; Crystal Optimisation for Numerical Absorption Correction;* Stoe & Cie GmbH: Darmstadt, Germany, 1999.
(83) Altomare, A.; Cascarano, G.; Giacovazzo, C.; Guagliardi, A. *J. Appl. Crystallogr.* **1993**, *26*, 343−350.
(84) Sheldrick, G. M. *Acta Crystallogr.* **2008**, *A64*, 112−122.
(85) Hübschle, C. B.; Sheldrick, G. M.; Dittrich, B. *J. Appl. Crystallogr.* **2011**, *44*, 1281−1284.